



Supporting Information

Sulfur-Containing Foldamer-Based Artificial Lithium Channels

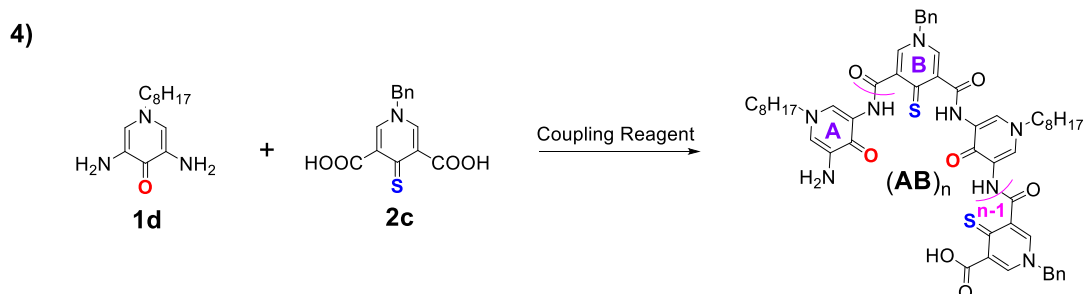
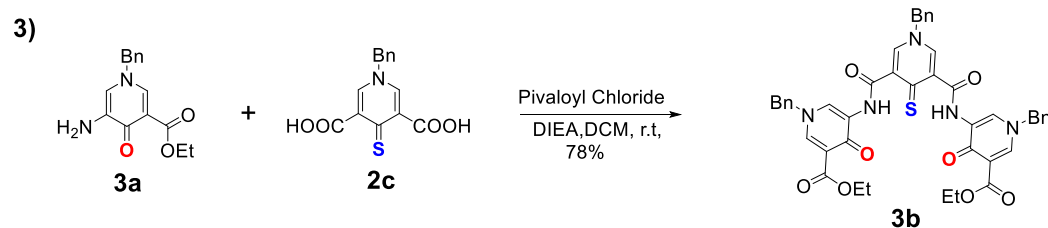
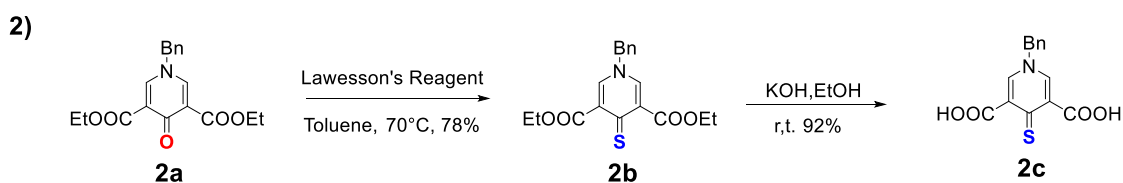
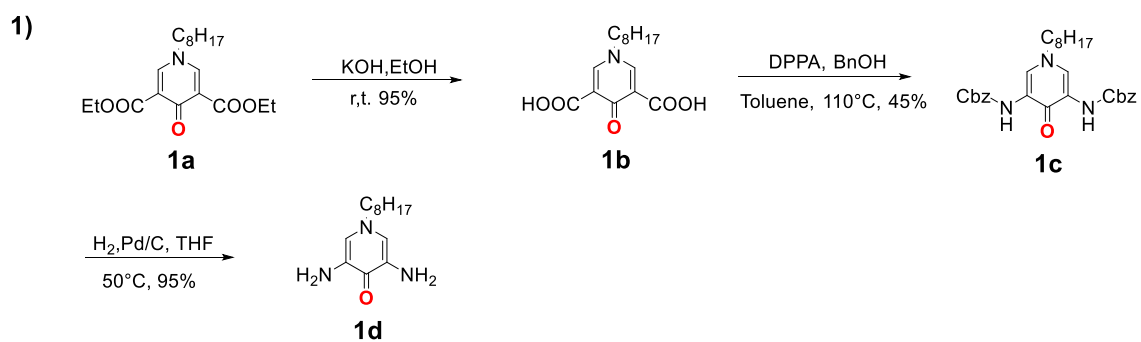
*J. Shen, D. R, Z. Li, H. Oh, H. Behera, H. Joshi, M. Kumar, A. Aksimentiev, H. Zeng**

1. General Remarks.....	S2
2. Scheme S1. Synthetic route that affords Lithium channels	S3
3. Synthetic Procedures & Characterization.....	S4
4. Molecular Weight Determination by GPC.....	S7
5. Molecular Weight Determination by ¹H NMR.....	S8
6. MALDI-TOF Distribution Patterns of the Polymers.....	S9
7. Ion Transport Study and the EC₅₀ Measurement Using the HPTS Assay	S10
8. The SPQ assay for anion selectivity.....	S12
9. Single Channel Current Measurement in Planar Lipid Bilayers.....	S13
10. Picrate extraction experiment for determination of binding constants.....	S17
11. Molecular Dynamics Simulation.....	S18
12. ¹H and ¹³C NMR Spectra.....	S27
13. References.....	S33

General Remarks

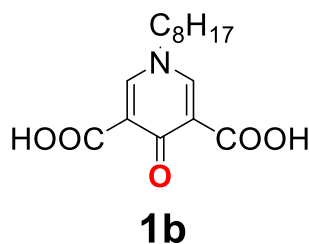
All the reagents were obtained from commercial suppliers and used as received unless otherwise noted. Aqueous solutions were prepared from MilliQ water. Flash column chromatography was performed using pre-coated 0.2 mm silica plates from Selecto Scientific. Chemical yield refers to pure isolated substances. ^1H and ^{13}C NMR spectra were recorded on Bruker ACF-400 spectrometer. The solvent signal of CDCl_3 was referenced at $\delta = 7.26$ ppm. The solvent signal of DMSO-d_6 was referenced at $\delta = 2.50$ ppm. Coupling constants (J values) are reported in Hertz (Hz). ^1H NMR data are recorded in the order: chemical shift value, multiplicity (s, singlet; d, doublet; t, triplet; q, quartet; m, multiplet; br, broad), number of protons that give rise to the signal and coupling constant, where applicable. ^{13}C spectra are proton-decoupled and recorded on Bruker ACF400 (400 MHz). The solvent, CDCl_3 , was referenced at $\delta = 77$ ppm. Solvent DMSO-d_6 was referenced at $\delta = 39.5$ ppm. CDCl_3 (99.8%-Deuterated) and DMSO-d_6 (99.8%-Deuterated) were purchased from Aldrich and used without further purification. Egg yolk phosphatidylcholine (EYPC) and 1,2-diphytanoyl-*sn*-glycero-3-phosphocholine (diPhyPC) used in this study were obtained from Avanti Polar Lipids. 4-(2-hydroxyethyl)-1-piperazineethanesulfonic acid (HEPES) buffer, 8-hydroxypyrene-1,3,6-trisulfonic acid (HPTS) dye, 6-methoxy-N-(3-sulfopropyl)quinolinium (SPQ) dye, Triton X-100, NaOH and all inorganic salts of molecular biology grade were purchased from Sigma. The ESI mass spectra were obtained by Thermo-Finnigan LCQ mass spectrometer. Fluorescence was recorded using fluorescence spectrophotometer (Hitachi, Model F7100, Japan).

Scheme S1. Synthetic route that affords lithium channels.

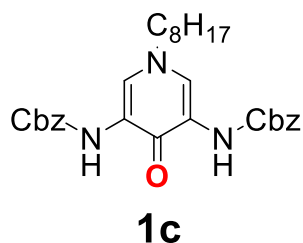


Synthetic Procedures & Characterization

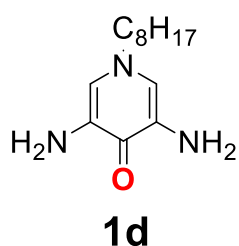
For synthesis of **1a,2a,3a** see: *J. Am. Chem. Soc.* **2011**, 133, 13930.



To a solution of **1a** (10.53 g, 30.0 mmol) in EtOH (150 mL) was added a solution of KOH (6.72 g, 120.0 mmol) in water, and the reaction was allowed to stir at room temperature for 24 hrs. After removing the solvent in vacuo, and dichloromethane (300 mL) was added, followed by addition of 1 M HCl aqueous solution (200 mL). The mixture was then stirred at room temperature for 30 min and organic layer was then collected with the aqueous layer further extracted using dichloromethane (3 × 200 mL). The combined organic layer was washed with brine and dried over Na₂SO₄. Dichloromethane was then removed in vacuo and the crude was purified by flash column chromatography to afford compound **1b** as a white solid. Yield: 8.4 g, 95%. ¹H NMR (400 MHz, DMSO-*d*₆) δ 14.30 (s, 2H), 8.87 (s, 2H), 4.25 (t, *J* = 7.4 Hz, 2H), 1.76 (p, *J* = 7.2 Hz, 2H), 1.30 – 1.19 (m, 10H), 0.88 – 0.81 (m, 3H). ¹³C NMR (101 MHz, DMSO) δ 176.82, 164.75, 148.28, 118.97, 58.09, 31.62, 30.77, 28.94, 28.84, 25.77, 22.51, 14.42. HR-ESI: calculated for [M+Na]⁺(C₁₅H₂₁NO₅Na): m/z 318.13, found: m/z 318.21.

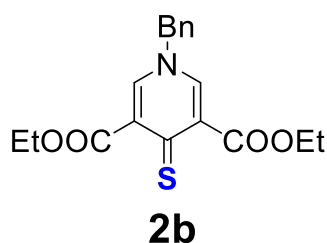


A suspension of **1b** (7.38 g, 25 mmol), DPPA (20.64 g, 75 mmol), TEA (13.9 ml, 100 mmol) and BnOH (15 ml) in Toluene (500 mL) was heated at 110 °C for 18 h. Removal of the solvent in vacuo gave the crude product, which was purified by flash column using EA/Hexane (1:1) to afford pure product **1c** as a white solid. Yield: 5.68 g, 45%. ¹H NMR (400 MHz, Chloroform-*d*) δ 8.42 (s, 2H), 7.91 (s, 2H), 7.42 – 7.30 (m, 10H), 5.19 (s, 4H), 3.88 (t, *J* = 7.5 Hz, 2H), 1.82 (s, 2H), 1.32 – 1.23 (m, 10H), 0.90 – 0.85 (m, 3H). ¹³C NMR (101 MHz, CDCl₃) δ 153.60, 135.35, 128.68, 128.49, 127.98, 67.88, 31.60, 31.17, 28.93, 28.85, 26.09, 22.55, 14.05. HR-ESI: calculated for [M+H]⁺(C₂₉H₃₆N₃O₅): m/z 506.26, found: m/z 506.38.

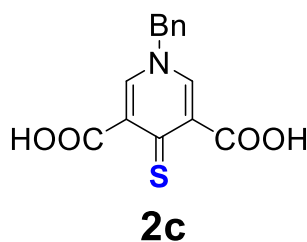


Compound **1c** (5.68 g, 11.24 mmol) underwent catalytic hydrogenation in THF (100 ml) at 55 °C for 10 hrs using Pd/C (0.57 g, 10 wt%) as the catalyst. The reaction was then filtered and the solvent was removed in vacuo to give the product **1d** as a brown oil. Yield: 2.53 g, 95%. ¹H NMR (400 MHz, DMSO-*d*₆) δ 7.01 (s, 2H), 4.27 (s, 4H), 3.75 (t, *J* = 7.0 Hz,

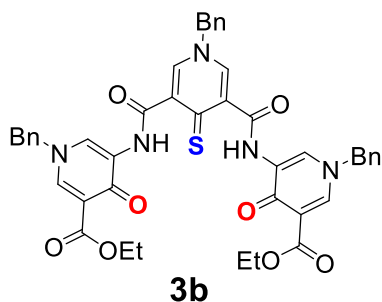
2H), 1.64 (p, $J = 7.1$ Hz, 2H), 1.22 (qt, $J = 9.0, 6.3, 4.9$ Hz, 10H), 0.87 – 0.82 (m, 3H). ^{13}C NMR (101 MHz, DMSO) δ 161.01, 134.20, 118.09, 56.85, 31.65, 31.01, 29.05, 29.01, 26.18, 22.52, 14.42. HR-ESI: calculated for $[\text{M}+\text{Na}]^+(\text{C}_{13}\text{H}_{23}\text{N}_3\text{ONa})$: m/z 260.17, found: m/z 260.20.



A suspension of **2a** (6.58 g, 20 mmol), and Lawesson's reagent (4.04 g, 10 mmol) in Toluene (200 mL) was heated at 70 °C for 24 h. The reaction was then filtered and removal of the solvent in vacuo gave the crude product, which was purified by flash column using EA/Hexane (1:2) to afford pure product **2b** as a yellow solid. Yield: 5.38 g, 78%. ^1H NMR (400 MHz, DMSO- d_6) δ 8.21 (s, 2H), 7.42 (s, 5H), 5.22 (s, 2H), 4.21 (q, $J = 7.1$ Hz, 4H), 1.25 (t, $J = 7.1$ Hz, 6H). ^{13}C NMR (101 MHz, DMSO) δ 184.22, 165.80, 137.04, 135.92, 135.84, 129.58, 129.24, 128.59, 61.57, 59.96, 14.38. HR-ESI: calculated for $[\text{M}+\text{H}]^+(\text{C}_{18}\text{H}_{20}\text{NO}_4\text{S})$: m/z 346.10, found: m/z 346.23.



The compound **2b** (5.38 g, 15.6 mmol) was dissolved directly in EtOH (40 ml), and KOH (2.62 g, 46.8 mmol) in water was added into the solution. The mixture was stirred at room temperature overnight and the solvent was then removed in vacuo. Water (100 ml), followed by addition of 1 M HCl aqueous solution (50 mL). The suspension was then filtered, washed by water (50 ml) and MeOH (20 ml). Then the residue obtained was dried to give a pure product **2c** as a yellow solid. Yield: 4.15 g, 78%. ^1H NMR (400 MHz, DMSO- d_6) δ 8.75 (s, 2H), 7.50 – 7.37 (m, 5H), 5.47 (s, 2H). ^{13}C NMR (101 MHz, DMSO) δ 181.39, 166.03, 140.55, 135.27, 133.83, 129.64, 129.47, 128.92, 60.92. HR-ESI: calculated for $[\text{M}+\text{H}]^+(\text{C}_{14}\text{H}_{12}\text{NO}_4\text{S})$: m/z 290.04, found: m/z 290.21.



In a 20 mL round bottomed flask protected with N_2 gas, compounds **2c** (0.2 mmol), Pivaloyl Chloride (0.4 mmol) and DIEA (N,N-Diisopropylethylamine, 75 μL) were dissolved in freshly distilled CH_2Cl_2 (10 mL) at r.t. for 2 hrs. **3a** (0.4 mmol), DIEA (N,N-Diisopropylethylamine, 75 μL) and distilled CH_2Cl_2 (2 mL) were added into the reaction mixture. The solution was then stirred at room temperature for 2 days. After

completion of reaction, solvent was evaporated to remove CH₂Cl₂. The obtained residue was recrystallized in cold MeOH to obtain the **3b** as yellow solid powder. Yield: 0.12 g, 78%. ¹H NMR (400 MHz, DMSO-*d*₆) δ 12.21 (s, 2H), 8.93 (d, *J* = 2.3 Hz, 2H), 8.71 (s, 2H), 8.59 (d, *J* = 2.3 Hz, 2H), 7.44 – 7.35 (m, 15H), 5.46 (s, 2H), 5.33 (s, 4H), 4.23 (q, *J* = 7.1 Hz, 4H), 1.28 (t, *J* = 7.1 Hz, 6H). ¹³C NMR (101 MHz, DMSO) δ 182.64, 166.99, 164.85, 163.25, 143.95, 141.15, 136.55, 135.52, 135.42, 132.51, 129.59, 129.55, 129.53, 129.33, 128.96, 128.94, 128.50, 128.43, 128.34, 127.67, 114.75, 60.72, 60.57, 60.22, 14.74. HR-ESI: calculated for [M+Na]⁺(C₄₄H₃₉N₅O₈SNa): *m/z* 820.24, found: *m/z* 820.31.

General procedure for one-pot synthesis of polymers:

In a 20 mL reaction vial protected with N₂ gas, compounds **1d** (0.2 mmol) and **2c** (0.2 mmol) were mixed, followed by adding coupling reagent (0.6 mmol), freshly distilled CH₂Cl₂ (10 mL) and anhydrous DMF (2 mL) and DIEA (N,N-Diisopropylethylamine, 150 μL). The solution was then stirred at room temperature for 2 days. After completion of reaction, solvent was evaporated to remove CH₂Cl₂ and DMF. The obtained residue was first washed with 10 mL MeOH/H₂O (1:1) and subsequently washed with 10 mL water and 10 mL MeOH and dried in oven (60 °C) to obtain polymers as yellow solid powder with yields of 35-42%. Average molecular weights (M_n) of all these polymers were determined by Gel Permeation Chromatography (GPC).

General protocol for synthesis of polymers with Pivaloyl Chloride: In a 20 mL round bottomed flask protected with N₂ gas, compounds **2c** (0.2 mmol), **Pivaloyl Chloride** (0.4 mmol) and DIEA (N,N-Diisopropylethylamine, 75 μL) were dissolved in freshly distilled CH₂Cl₂ (10 mL) at r.t. for 2 hrs. **1d** (0.2 mmol), DIEA (N,N-Diisopropylethylamine, 75 μL) and anhydrous DMF (2 mL) were added into the reaction mixture. The solution was then stirred at room temperature for 2 days. After completion of reaction, solvent was evaporated to remove CH₂Cl₂ and DMF. The obtained residue was first washed with 10 mL MeOH/H₂O (1:1) and subsequently washed with 10 mL water and 10 mL MeOH and dried in oven (60 °C) to obtain polymers as yellow solid powder with yields of 67%. Average molecular weights (M_n) of all these polymers were determined by Gel Permeation Chromatography (GPC).

Molecular Weight Determination by GPC

Gel Permeation Chromatography (GPC) analyses for polymer products were carried out with a Shimadzu Prominence Liquid Chromatograph system (LC-20AR) equipped with a communications bus module (CBM-20A) with two Styragel[®] HR 1 and HR 4E DMF columns (size: 300 × 7.8 mm) in series and a Shimadzu RID-20A refractive index detector. The mobile phase used was DMF with a flow rate of 1 mL/min. Number-averaged molecular weights were calculated from a calibration curve using a series of poly(ethylene glycol) standards with molecular weights ranging from 633 to 20,600 Da.

Polymer samples (5 mg/mL, 1 mL) were prepared in commercially available HPLC grade DMF (degassed for 15 min before use). The prepared samples were filtered through PTFE Syringe Filter (0.45 μm) before running for GPC with auto sampler.

Table S1. Molecular weights (M_n , Da) of polymers P_n produced using different types of coupling agents.^a

Coupling Reagents ^a	M_n (KDa)	PDI
HATU	< 3000	-
HBTU	< 3000	-
BOP	< 3000	-
PyBOP	< 3000	-
Pivaloyl Chloride	7599	1.05

^a HATU = 1-[Bis(dimethylamino)methylene]-1H-1,2,3-triazolo[4,5-b]pyridinium 3-oxide hexafluorophosphate, HBTU = 2-(1H-benzotriazol-1-yl)-1,1,3,3-tetramethyluronium hexafluorophosphate, BOP = benzotriazol-1-yloxytris(dimethylamino)phosphonium hexafluorophosphate, PyBOP = benzotriazol-1-yloxytripyrrolidinophosphonium hexafluorophosphate.

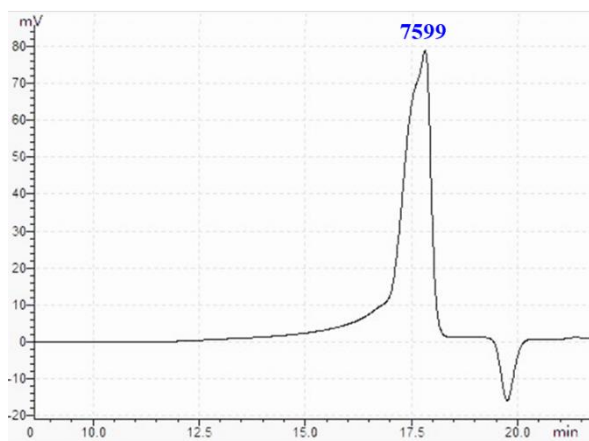
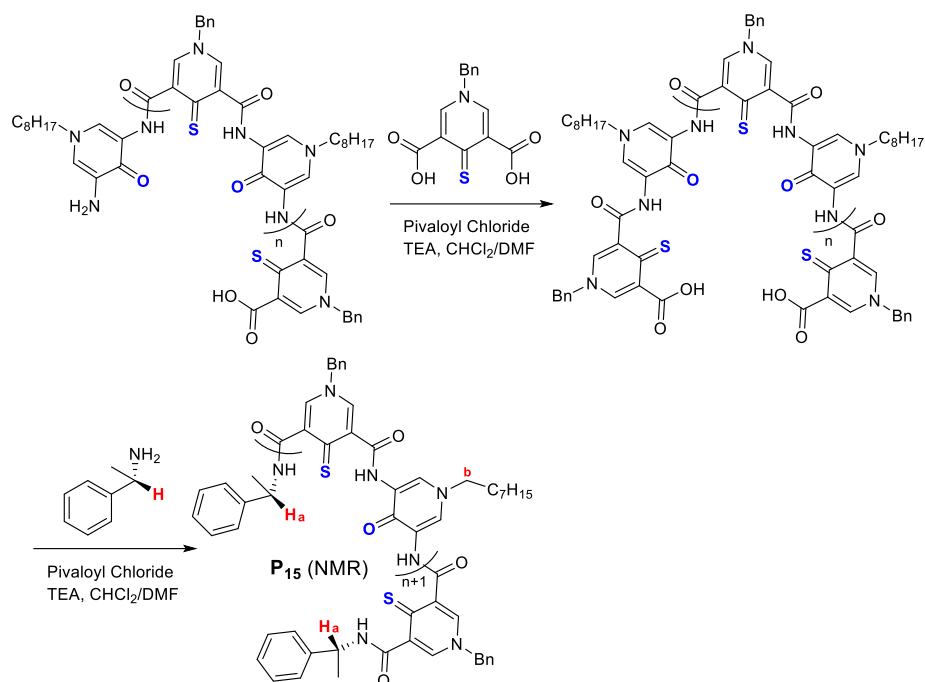


Figure S1. GPC data for polymeric channel P_{15} generated using pivaloyl chloride

Molecular Weight Determination by ^1H NMR



Scheme S2. Synthesis of polymers P_{15} (NMR) having an internal NMR standard (H_a from the end C-H bond) for molecular weight determination using the ^1H NMR spectrum.

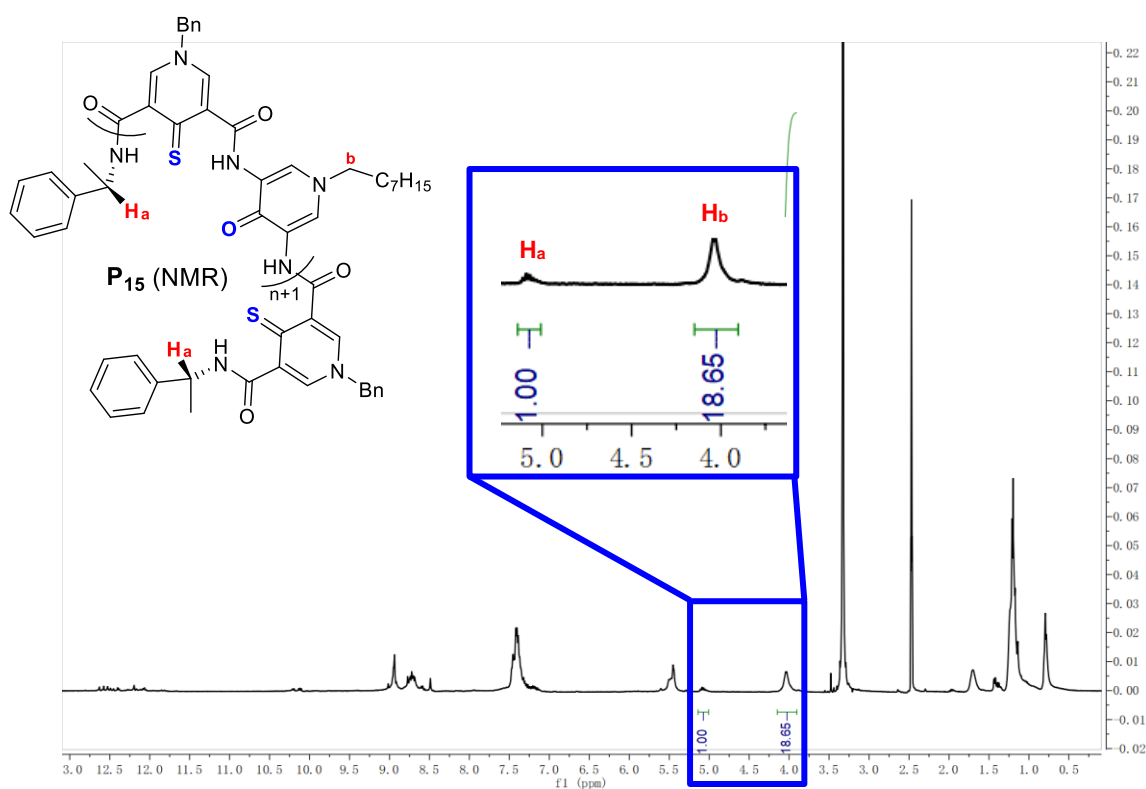


Figure S2. From NMR peak areas of H_a and H_b , the average number of repeating units of P_{15} (NMR) was determined to be 18.65, which compares well with the 15.45 units determined using GPC.

MALDI-TOF Distribution Patterns of the Polymers

MALDI-TOF mass spectra were acquired with Bruker Ultraflexreme (Bruker Daltonik GmbH, Germany) equipped with Bruker smartbeam II 355 nm nitrogen laser with an accelerating voltage of 25 kV in the linear configuration. Mass spectra were measured by using the positive mode of mass spectroscopy. The matrix used in the experiment was trans-2-[3-(4-tertButylphenyl)-2-methyl-2-propenylidene]malononitrile (DCTB) from TCI and used directly without further purification. The solid matrix was dissolved in chloroform at 10 mg/mL. 10 μ L of matrix solution was then spotted onto the MALDI sample plate, followed by addition of 5 μ L of the chloroform solution of polymers (1 mg/mL). Sample was air-dried at room temperature. The dried plate was inserted into the MALDI instrument that can detect up to 10,000 Da. Selection of the laser used for ionization was performed directly through the software and required no adjustments to the individual lasers. Polymers displayed characteristic mass pattern of repeating unit in the MALDI spectra. The highly electron-rich interior of helical channel can be protonated or bind to Na^+ or K^+ ions, producing doubly or multiply charged species in the MALDI spectra.

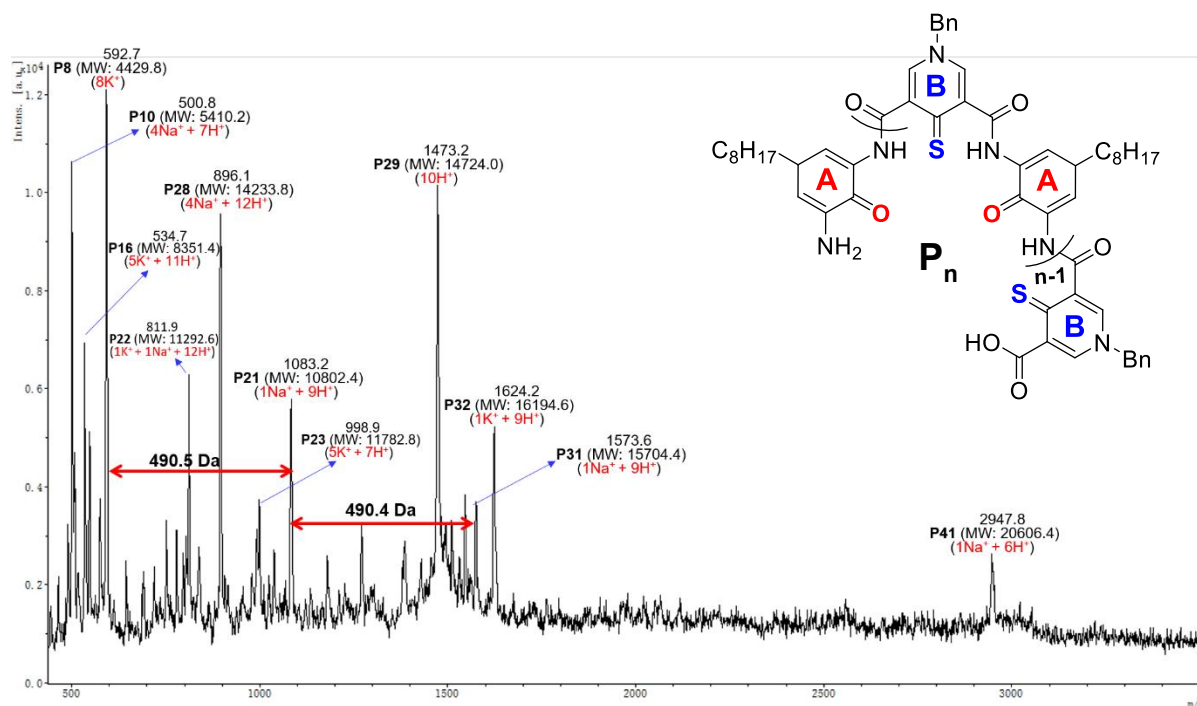


Figure S3. MALDI-TOF pattern of polymer-based channel P15.

Ion Transport Study and the EC50 Measurement Using the HPTS Assay

EYPC (1 ml, 25 mg/mL in CHCl₃, Avanti Polar Lipids, USA) was added in a round-bottom flask. The solvent was removed under reduced pressure at 30 °C. After drying the resulting film under high vacuum overnight, the film was hydrated with a HEPES buffer solution (1 mL, 10 mM HEPES, 100 mM NaCl, pH = 7.0) containing a pH sensitive HPTS dye (1 mM) at room temperature for 60 minutes to give a milky suspension. The mixture was then subjected to 10 freeze-thaw cycles: freezing in liquid N₂ for 1 minute and heating 55 °C water bath for 2 minutes. The vesicle suspension was extruded through polycarbonate membrane (0.1 μm) to produce a homogeneous suspension of large unilamellar vesicles (LUVs) of about 120 nm in diameter with HPTS encapsulated inside. The unencapsulated HPTS dye was separated from the LUVs by using size exclusion chromatography (stationary phase: Sephadex G-50, GE Healthcare, USA, mobile phase: HEPES buffer with 100 mM NaCl) and diluted with the mobile phase to yield 5 mL of 6.5 mM lipid stock solution.

The HPTS-containing LUV suspension (15 μL, 6.5 mM in 10 mM HEPES buffer containing 100 mM NaCl at pH = 7.0) was added to a HEPES buffer solution (1.95 mL, 10 mM HEPES, 100 mM MCl at pH = 8.0, where M⁺ = Li⁺, Na⁺, K⁺, Rb⁺, and Cs⁺) to create a pH gradient for ion transport study. A solution of channel molecules in DMSO was then injected into the suspension under gentle stirring. Upon the addition of channels, the emission of HPTS was immediately monitored at 510 nm with excitations at both 460 and 403 nm recorded simultaneously for 300 s using fluorescence spectrophotometer (Hitachi, Model F-7100, Japan) after which time an aqueous solution of Triton X-100 was immediately added to achieve the maximum change in dye fluorescence emission. The final transport trace was obtained, after subtracting background intensity at t = 0, as a ratiometric value of I₄₆₀/I₄₀₃ and normalized based on the ratiometric value of I₄₆₀/I₄₀₃ after addition of triton. The fractional changes R_{Li⁺} was calculated for each curve using the normalized value of I₄₆₀/I₄₀₃ at 300 s before the addition of triton, with triton with ratiometric value of I₄₆₀/I₄₀₃ at t = 0 s as 0% and that of I₄₆₀/I₄₀₃ at t = 300 s (obtained after addition of triton) as 100%. Fitting the fractional transmembrane activity R_{Li⁺} vs channel concentration using the Hill equation gave the Hill coefficient *n* and EC₅₀ values:

$$Y = 1/(1 + (EC_{50}/[C])^n)$$

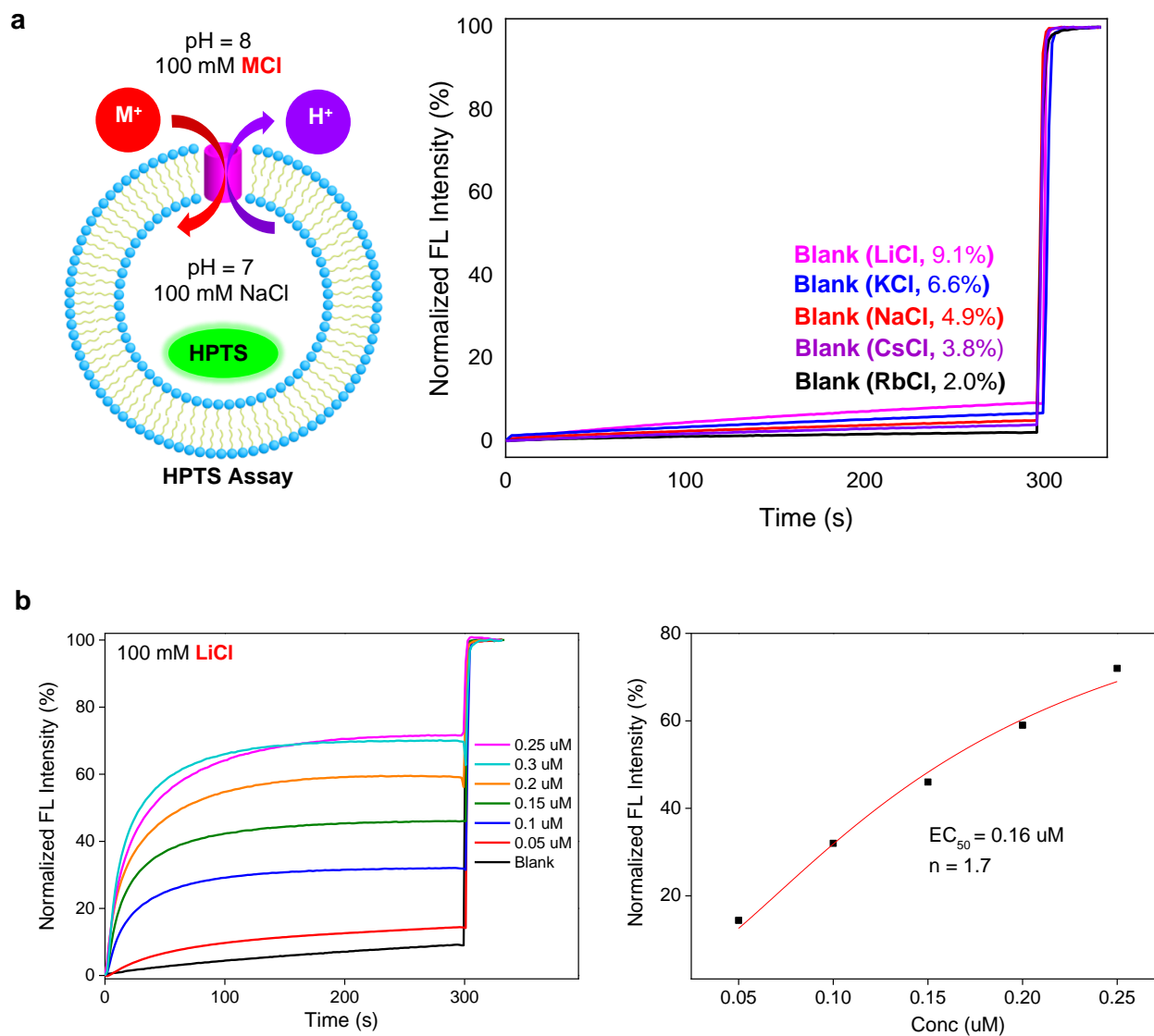


Figure S4. a) The background signals in the presence of varied MCl in the extracellular region of the LUVs. b) Determination of EC_{50} value of $0.16 \mu\text{M}$ (or 0.32 mol\% relative to lipid) for channel P_{15} using the Hill analysis.

The SPQ assay for anion selectivity

The SPQ-containing LUV suspension (25 μL , 4 mM in 200 mM NaNO_3) was added to a solution (1.95 mL, 200 mM NaCl) to create anion concentration gradients for ion transport study. A solution of channel in DMSO was then injected into the suspension under gentle stirring. Upon the addition of channels, the emission of SPQ was immediately monitored at 440 nm with excitations at 380 nm for 300 s using fluorescence spectrophotometer (Hitachi, Model F-7100, Japan) after which time an aqueous solution of Triton X-100 (20 μL , 20% v/v) was immediately added to destroy the chloride gradient. The final transport trace was obtained by normalizing the fluorescence intensity using the following equation,

$$I_F = [(F_t - F_0)/(F_\infty - F_0)]$$

Where F_0 = Fluorescence intensity just before the compound addition (at $t = 0$ s), F_t = Fluorescence intensity at time t , and F_∞ = Fluorescence intensity at saturation after complete leakage (at $t = 300$ s).

Single Channel Current Measurement in Planar Lipid Bilayers

The chloroform solution of diPhyPC (10 mg/ml, 20 μ L) was evaporated using nitrogen gas to form a thin film and re-dissolved in *n*-decane (8 μ L). 0.2 μ L of this *n*-decane solution was injected into the aperture (diameter = 250 μ m) of the Delrin[®] cup (Warner Instruments, Hamden, CT) with the *n*-decane removed using nitrogen gas. In a typical experiment for conductance measurement, both the chamber (*cis* side) and Delrin cup (*trans* side) were filled with an aqueous LiCl solution (1.0 M, 1.0 mL). Ag-AgCl electrodes were inserted into the two solutions with the *cis* chamber grounded. Planar lipid bilayer was formed by painting 0.3 μ L of the lipid-containing *n*-decane solution around the *n*-decane-pretreated aperture. Successful formation of planar lipid bilayers can be established with a capacitance value ranging from 80-120 pF. Then at each time, 0.1 μ L of sample in THF was added to the *cis* compartment and the solution was stirred for 20 s. After 5 to 10 times, a single current trace appeared. And the final concentration of the sample was around 10^{-8} M. These single channel currents were then measured using a Warner BC-535D bilayer clamp amplifier, collected by PatchMaster (HEKA) with a sample interval at 5 kHz and filtered with an 8-pole Bessel filter at 1 kHz (HEKA). The data were analysed by FitMaster (HEKA) with a digital filter at 100 Hz.

For the measurement of the transport selectivity of Li^+ over M^+ , the *cis* chamber was charged with LiCl (1.0 M) and the *trans* one was charged with MCl (1.0 M, $\text{M} = \text{Na}^+$ and K^+). The selectivity of the channels for Li^+ over M^+ , defined as the permeability ratio of two ions, was calculated by using the simplified Goldman–Hodgkin–Katz equation:

$$\varepsilon_{\text{rev}} = \frac{RT}{F} \times \ln\left(\frac{P_{\text{M}^+ \text{trans}}}{P_{\text{Li}^+ \text{cis}}}\right)$$

where ε_{rev} is the reversal membrane potential; R is the universal gas constant ($8.314 \text{ J}\cdot\text{K}^{-1}\cdot\text{mol}^{-1}$); T the temperature in Kelvin (298 K); F is the Faraday's constant ($96485 \text{ C}\cdot\text{mol}^{-1}$); P is the permeability of the channel for ions.

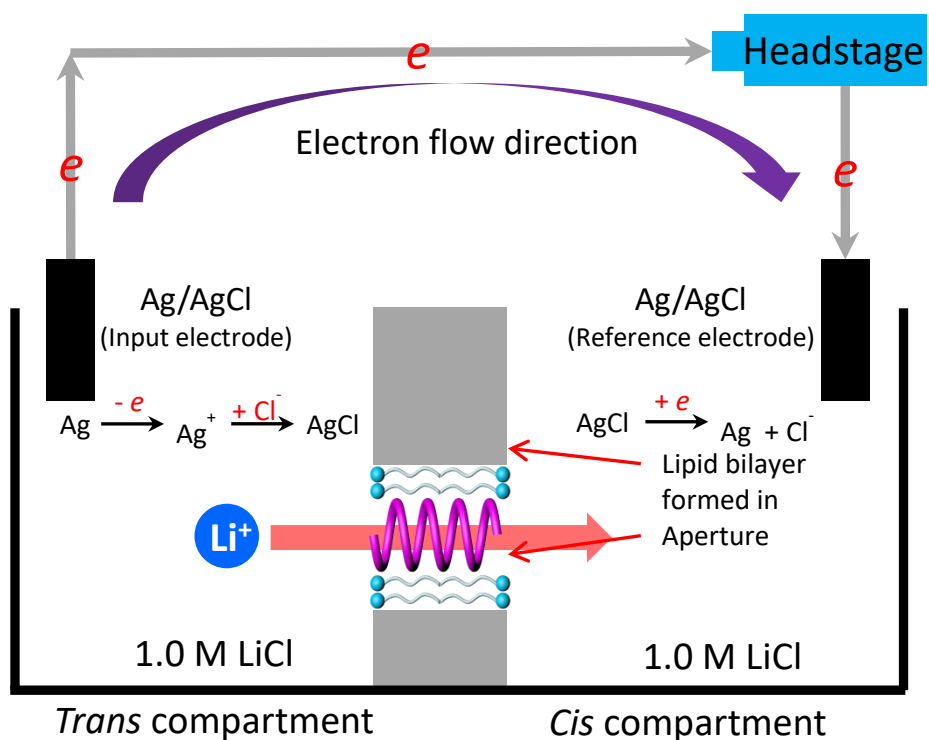


Figure S5. Schematic illustration of the experimental setup for determining values of lithium conductance (γ_{Li^+}). Redox reaction schemes on both Ag/AgCl electrodes were used to highlight the charge balance during Li^+ transport. For measurement of Li^+/M^+ transport selectivity, 1.0 M LiCl in trans chamber was replaced by 1.0 M MCl (M = Na and K).

Li⁺/Na⁺ selectivity

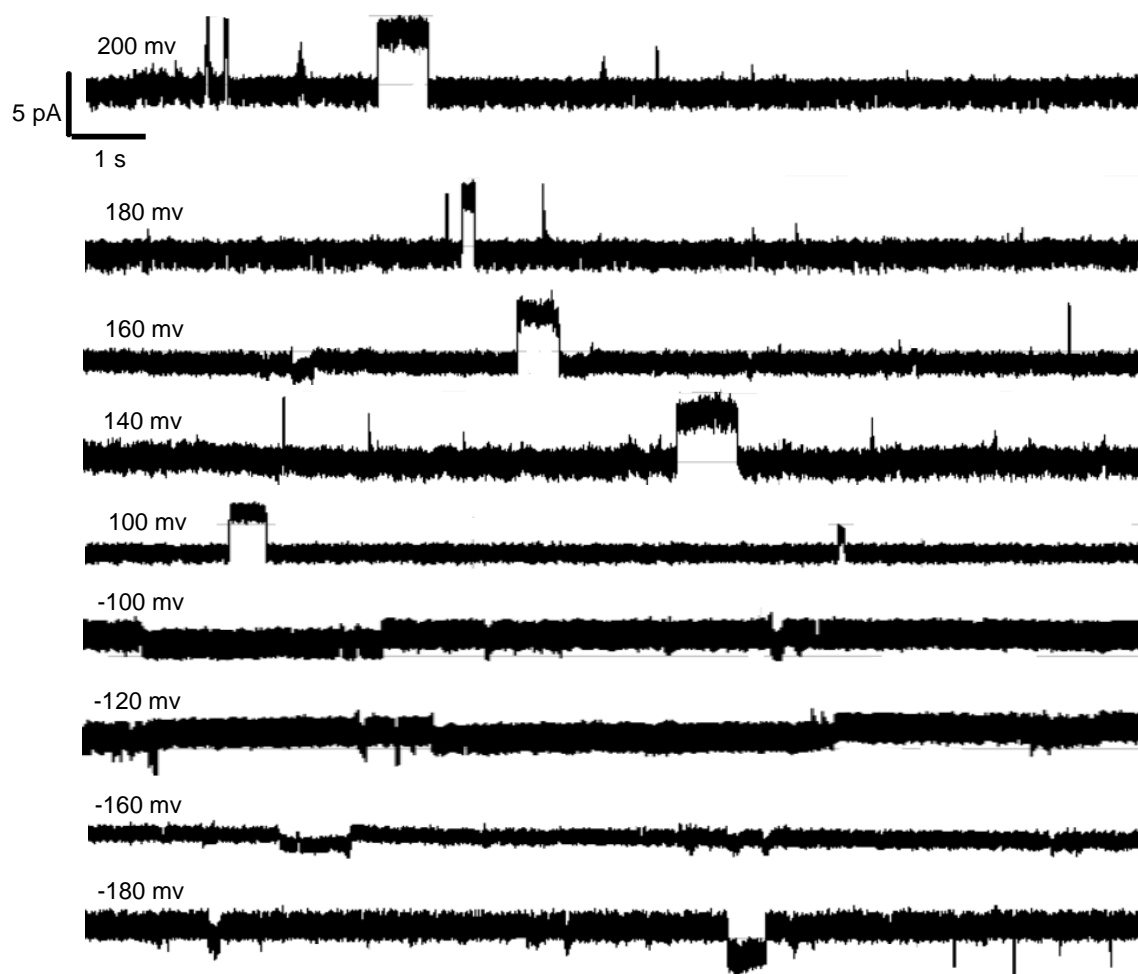


Figure S6. Single channel currents recorded for **P15**, with *cis* chamber having 1.0 M LiCl and *trans* chamber having 1.0 M LiCl for determining Li⁺/Na⁺ selectivity ($P_{\text{Li}^+}/P_{\text{Na}^+} = 15.3 \pm 1.1$).

Li⁺/K⁺ selectivity

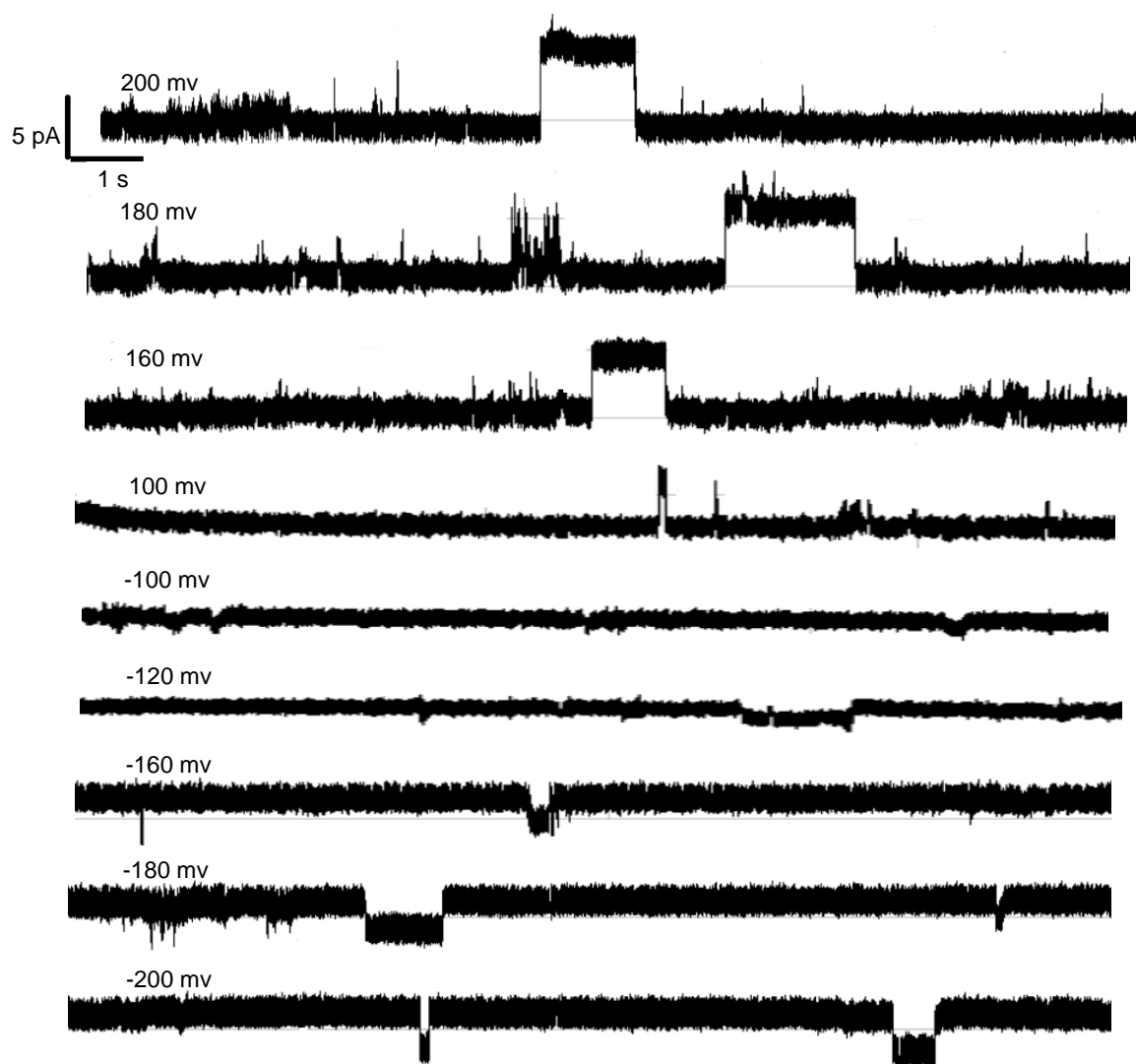


Figure S7. Single channel currents recorded for **P15**, with *cis* chamber having 1.0 M LiCl and *trans* chamber having 1.0 M KCl for determining Li⁺/K⁺ selectivity ($P_{Li^+}/P_{K^+} = 19.9 \pm 1.1$).

Picrate extraction experiment for determination of binding constants

Preparation of alkali metal picrates: The sodium and potassium picrates were prepared by dissolving picric acid in a minimum amount of distilled boiling water and slowly adding a stoichiometric amount of the alkali metal hydroxide. The alkali metal picrate solution was cooled to room temperature and placed in an ice bath to facilitate crystallization. The precipitate was filtered and recrystallized from distilled water. After filtration and extensive air drying, the salt was carefully heated to dryness in a vacuum oven at 75°C for overnight and cooled to room temperature under N₂ protection. The anhydrous metal picrates were stored in a desiccator.

Procedure for picrate extraction experiment for determining association constant between channel molecules and Na⁺ or K⁺ : Extractions of sodium or potassium picrates with channels were performed by placing 1.0 mL of a 10 mM solution of the metal picrate in deionized water and 1.0 mL of a 10 mM solution of the channels in chloroform into a 4-mL sample vial and mixing the solutions on a vortex mixer for 60 seconds. The sample was then allowed to stand for 30 minutes to ensure a complete separation of the layers. Aliquot was taken from the aqueous phase of the sample, and the concentration of metal picrate in aqueous phase was determined by UV-Visible spectroscopy with a scanning from 300 nm to 500 nm. The association constants K_a were calculated according to method previously described (Moore, S. S.; Tarnowski, T. L.; Newcomb, M.; Cram, D. J. *J. Am. Chem. Soc.* **1977**, *99*, 6398-6405). Three samples were prepared for each picrate extraction experiment. Standard deviations from the analysis of the three samples were less than 10% in terms of the K_a values.

Table S2. Binding constants (K_a) between **P**_{1.5} and alkali metal ions (Li, Na⁺, K⁺, Rb⁺ and Cs⁺ ions) at 25 °C obtained by Cram's method.^[a]

	R	K_a (M ⁻¹) ^[b]
Li ⁺	0.058	$(0.89 \pm 0.01) \times 10^3$
Na ⁺	0.040	$(3.90 \pm 0.06) \times 10^3$
K ⁺	0.060	$(4.00 \pm 0.05) \times 10^3$
Rb ⁺	0.040	$(1.79 \pm 0.03) \times 10^3$
Cs ⁺	0.078	$(1.93 \pm 0.02) \times 10^3$

[a] [Guest]/[host] ratio in CHCl₃ layer at equilibrium. For reference, see: Moore, S. S.; Tarnowski, T. L.; Newcomb, M.; Cram, D. J. *J. Am. Chem. Soc.* **1977**, *99*, 6398-6405. [b] Averaged values over three runs with the assumption of 1:1 guest/host binding stoichiometry.

Molecular dynamics simulations revealing the molecular basis of Li⁺ selectivity of P₁₅ channel

To visualize and understand the molecular level structure and Li⁺ ions selectivity of the P₁₅ channel, we performed all-atom simulations using NAMD2 program.¹ Based on the crystal structure of P_{1.5} (Figure 1b), we built an all-atom model of the P₁₅ channel (Figures 1c, 4a and S7a-b as well as Supplementary Video SV1) and solvated it in a 0.5 M aqueous solution of LiCl. Two simulation systems were created by adding 0.5 M KCl (System 1) or 0.5 M NaCl (System 2), respectively. The overall structure and the diameter (~ 3.6 Å) of P₁₅ largely remain unchanged at the end of 1 μs long equilibrium simulations without any restraints (Figure S7c-d and Supplementary Video SV2).

Owing to its smallest hydration shell comprising 4 water molecules² as compared to the other alkali metal ions, the hydrated Li⁺ ion fits well inside the P₁₅ channel (Figures 4b and S8). Within the first few nanoseconds of the MD simulations in both Systems 1 and 2, we observed that Li⁺ ions readily enter P₁₅ and that there are always two Li⁺ ions residing inside P₁₅ during the whole 1 μs long MD simulations (Figure S7e). In contrast, no Cl⁻ ions ever enter the channel. Occasionally, some Na⁺ ions also entered the channel (Figure S7f). The average density of Li⁺ ions measured inside the channel is far more than one order of magnitude higher than both Na⁺ and K⁺ ions (Figure 4e-f). Interestingly in the presence of KCl, the hydrated Li⁺ ions stabilized the channel structure slightly better than NaCl system via the formation of long-lasting H-bonds between the H-atoms of water molecules and O-atoms from the channel wall (Figure 4b-c). The average number of water molecules present inside the channel turns out to be ~ 15 and 19 in system 1 and system 2 (Figure S9), respectively. By forming H-bonds with the inner walls of the P₁₅ channel (Figure S10), the water molecules present inside the channel compensate the lost hydrogen bonds due to confinement from the narrow cavity. Li⁺ ions inside the channel appears to form a hexagonal coordination with the sulfur atoms present on the channel wall (Figure S11). Thus, our equilibrium simulations strongly suggest that the small pore size of P₁₅ appears to be ideal fit for permeating the Li⁺ ions, while sterically excluding the Cl⁻ ions and the other larger alkali metal ions such as Na⁺ and K⁺.

To further investigate the Li⁺ selectivity, we have performed free energy calculations using the replica exchange umbrella sampling (REUS) method³ (Figure 4d). The computed high free energy barrier for Cl⁻ ions certainly prevents these anions from entering P₁₅. Corroborated further by the “knock-on” mechanism (Supplementary Video SV2), the consistently more

negative free energies of Li⁺ ions as compared to those for the K⁺ and Na⁺ ions explain the highly selective permeation of Li⁺ ions through **P15**.

Method and Materials

General MD protocol: All MD simulations were performed using the MD simulation program NAMD2¹, periodic boundary conditions and particle mesh Ewald (PME) method to calculate the long range electrostatics⁴. The Nose-Hoover Langevin piston^{5, 6} and Langevin thermostat⁷ were used to maintain the constant pressure and temperature in the system. CHARMM36 force field parameters⁸ described the bonded and non-bonded interactions of among, lipid bilayer membranes, water and ions. We used the standard CHARMM ion parameters by Roux and coworkers⁹ with CUFIX^{10, 11} corrections for describing the non-bonded interaction of Li⁺, K⁺, Na⁺ and Cl⁻ ions in the system. A 8-10-12 Å cutoff scheme was used to calculate van der Waals and short range electrostatics forces. All simulations were performed using a 2 fs time step to integrate the equation of motion. SETTLE algorithm¹² was applied to keep water molecules rigid whereas RATTLE algorithm¹³ constrained all other covalent bonds involving hydrogen atoms. The coordinates of the system were saved at an interval of 19.2 ps. The analysis and post processing the simulation trajectories were performed using VMD¹⁴ and CPPTRAJ¹⁵.

All-atom model of P15 channel: The initial structure of **P15** channel consisting of 15 **AB** type repeating units was built based on the bond angles and lengths of the crystal structure of a short oligomer (Figure 1b). This was followed by applying the geometrical transformations using a custom VMD script (Figure S7 and Supplementary Movie SV1). The topology and force field parameters for one unit of the **P15** channel was obtained using the CHARMM general force fields (CGenFF) webserver.¹⁶ The protein structure file (psf) of the **P15** molecule was constructed using the psfgen tool of VMD.

Simulation of ion permeation through P15 channel in aqueous solution: The all-atom model of **P15** channel was solvated with TIP3P water molecules using the Solvate plugin of VMD. Lithium and chloride ions were added to 0.5 M concentration of LiCl₂ in the system using the Autoionize plugin of VMD. Finally, we created two systems by adding potassium chloride (system 1) or sodium chloride (system 2) to have 0.5 M concentration of KCl or NaCl. Thus, assembled systems measured 6 x 6 x 6 nm³ and contained approximately 20,000 atoms (Figure 4a). Following the assembly, the system underwent 1200 steps of energy minimization using the conjugate gradient method to remove steric clashes. After energy minimization, the system was subjected to a 170 ns equilibration at a constant number of atoms (N), pressure (P

= 1 bar) and temperature ($T = 300$ K), the NPT ensemble, with harmonic restraints applied to all heavy atoms of the channel around the pore. The restraints were applied relative to the initial coordinates of the atoms having the spring constants of $1 \text{ kcal mol}^{-1} \text{ \AA}^{-2}$. Subsequently the harmonic restraints were reduced to 0.1, 0.01 $\text{kcal mol}^{-1} \text{ \AA}^{-2}$ value of spring constant for next 10 ns seconds. Finally, $\sim 1\mu\text{s}$ long production MD simulations were performed without any restraints.

Free energy calculations: To calculate the free energy profile of an ion passing through the central lumen of the **P15** channel, we employed the replica exchange umbrella sampling (REUS) technique¹⁷ implemented within the *colvar* module of NAMD³. Taking the last snapshot of the 200 ns equilibrated system in electrolyte solution (during which the non-hydrogen atoms of the channel around the pore were harmonically restrained), we created 31 copies of each of the system by pulling a single ion along the axis of the channel in a 120 ns long steered molecular dynamics run. *distanceXY* colvar with radius 3 \AA (shown using a cylinder around the **P15** channel in the Figure 4a) was used to make sure that the ion passes through the constriction of the channel. We chose the snapshot of the system where the ion falls in the respective sampling window of the 1 \AA bin along the Z axis and harmonically restrained it to the center of the window. The spring constant of the harmonic potential was $2.5 \text{ kcal/mol/ \AA}^2$. Each replica was simulated for 130 ns and the replicas were allowed to exchange with a probability given by the Metropolis algorithm. Finally, we used WHAM¹⁸ program to subtract the contribution from the confining harmonic potential and extracted the potential of mean force (PMF) of ion along the axis of the channel.

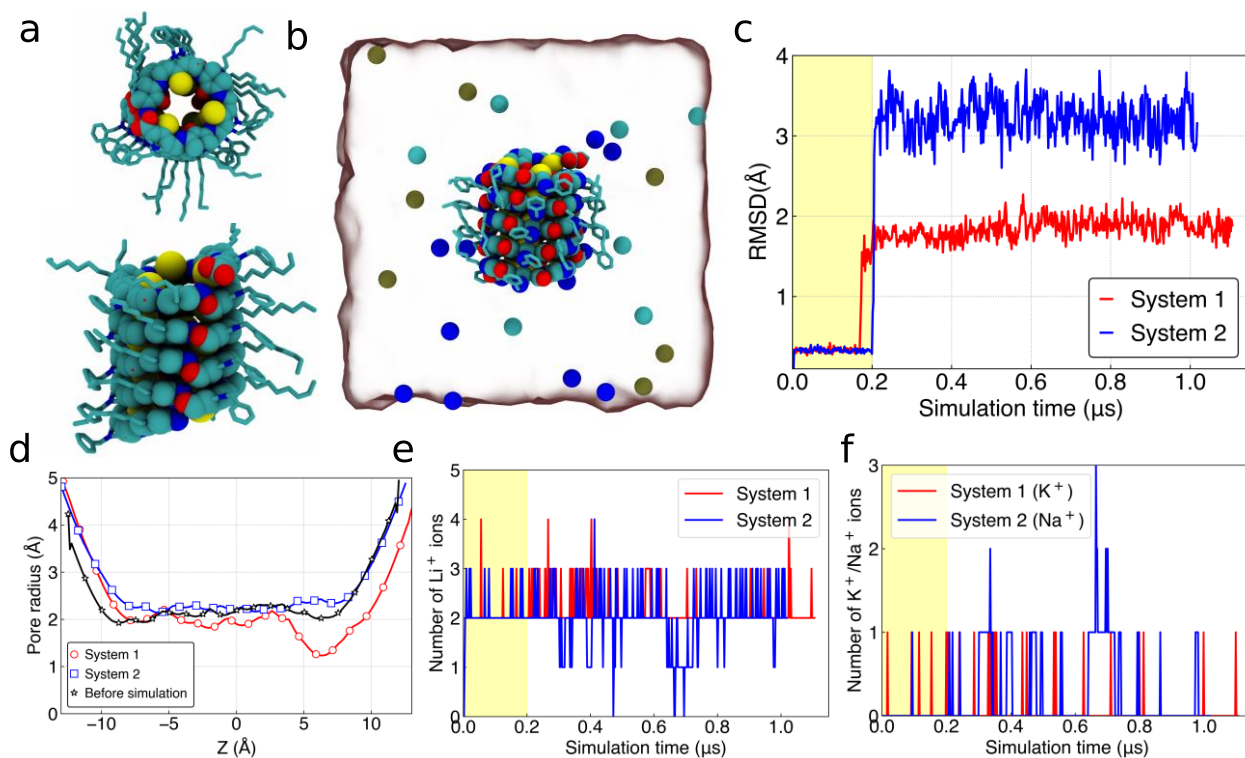


Figure S8: MD simulation of water and ion transport through the P₁₅ channel in aqueous environment. (a) Top and side view of the all-atom model of P₁₅ channel, the non-hydrogen atoms surrounding the pore are shown using cyan (C), red (O), blue (N) and yellow (S) spheres whereas the side chains are shown using licorice representation. (b) Representative snapshot of a P₁₅ channel immersed in box of water (semitransparent white background) and ions. (c) Root mean square deviation (RMSD) of the channels as a function of simulation time. The yellow shaded region shows the time when channels were restrained using harmonic constraints. (d) The radius of the channel at the beginning and end of the simulations in system 1 and system 2 computed using HOLE program¹⁹. (e) The number of Li⁺ and (f) total number of K⁺ (system 1) or Na⁺ (system 2) ions present inside the P₁₅ channel as a function of simulation time.

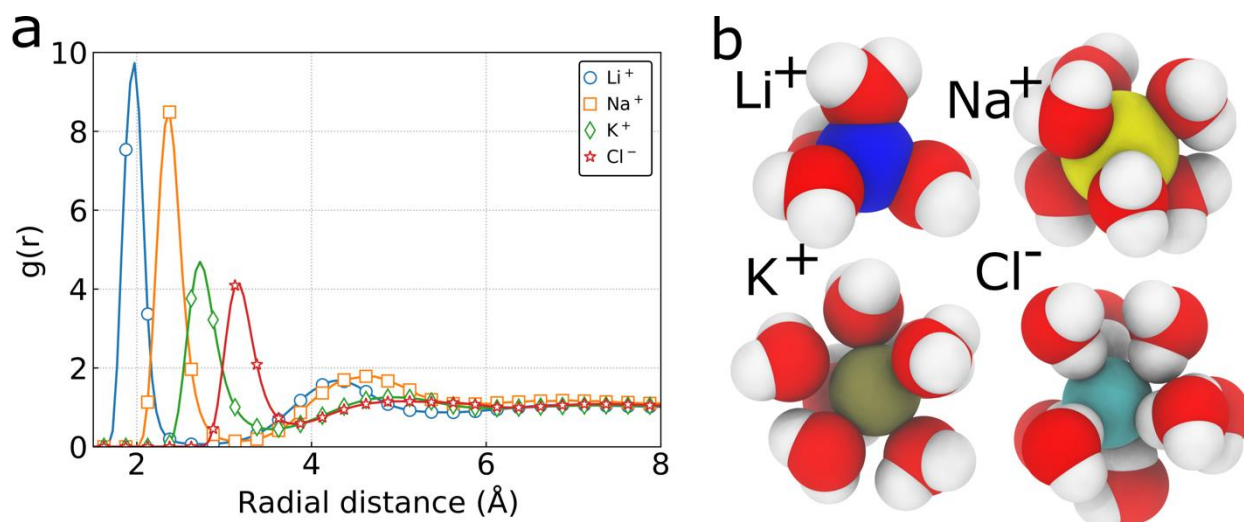


Figure S9: Radial distribution function and hydration shell of ions. (a) RDF of various ions obtained from the equilibrium MD simulation trajectories. Based on the first minima in RDF, we define the radius of the first hydration shell for Li^+ , Na^+ , K^+ , and Cl^- as 2.8 Å, 3.2, 3.5 Å and 3.8 Å respectively. (b) An instantaneous snapshot illustrating various ions and their first hydration shell in bulk during the all-atom MD simulations.

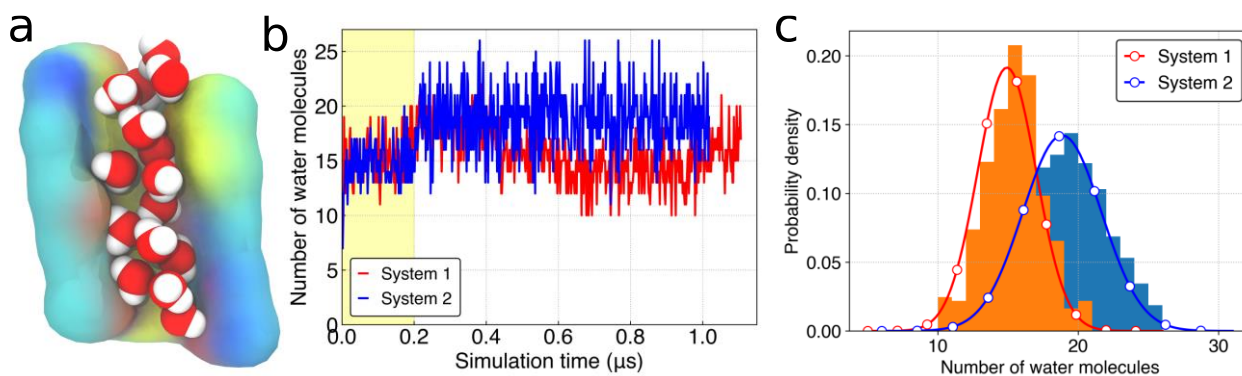


Figure S10: Water wires inside the P_{15} channel in simulation. (a) A representative snapshot of the system illustrating the water molecules inside the P_{15} channel. (b) The number of water molecules inside the P_{15} channel as a function of simulation time. (c) The probability density of the water molecules present inside the channel, the solid line shows a normal fit to the distribution peaking at ~ 15 and ~ 19 molecules for system 1 and system 2 respectively.

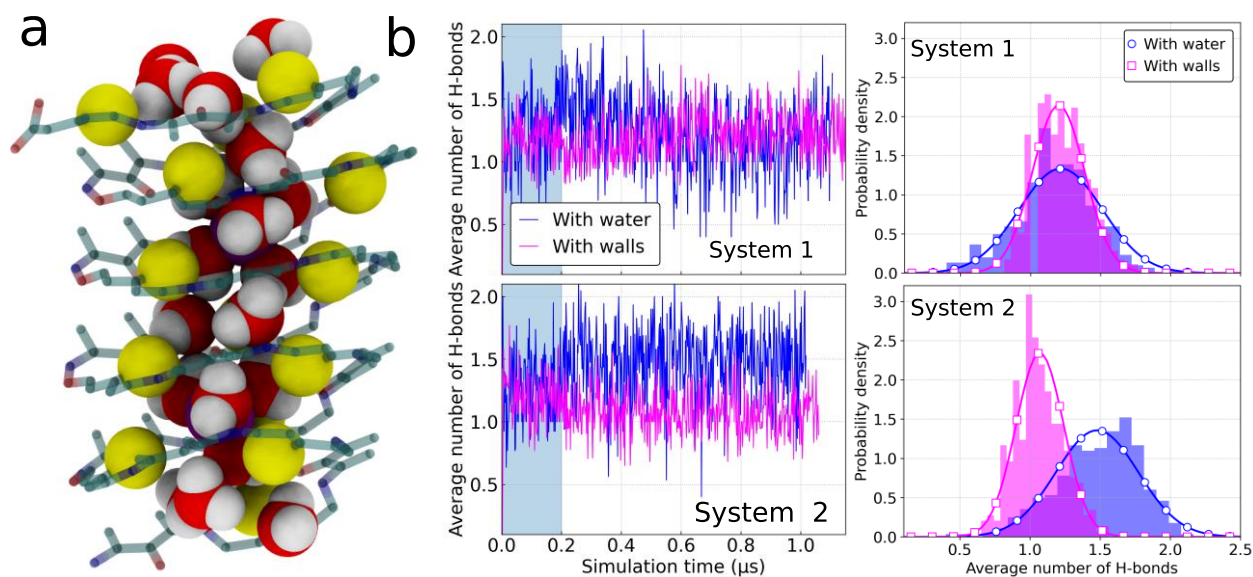


Figure S11: H-bonds of water molecules inside the channel. (a) A representative snapshot of the system illustrating the water molecules inside the \mathbf{P}_{15} channel, sulfur atoms of the channel are highlighted as yellow spheres, the side chain of the channel are not shown. (b) The average number of H-bonds formed by a water molecule present inside the \mathbf{P}_{15} channel with the other water molecules in the vicinity and those with the atoms of the inner walls of the \mathbf{P}_{15} channel. The probability distribution (excluding the first 200 ns) of h-bonds is shown on the left. As compared to the system 2 (bottom row), in system 1 (top row) where the Li^+ form long lasting contacts with the channel, the average number of h-bonds formed by the water molecule with the channel walls also increased.

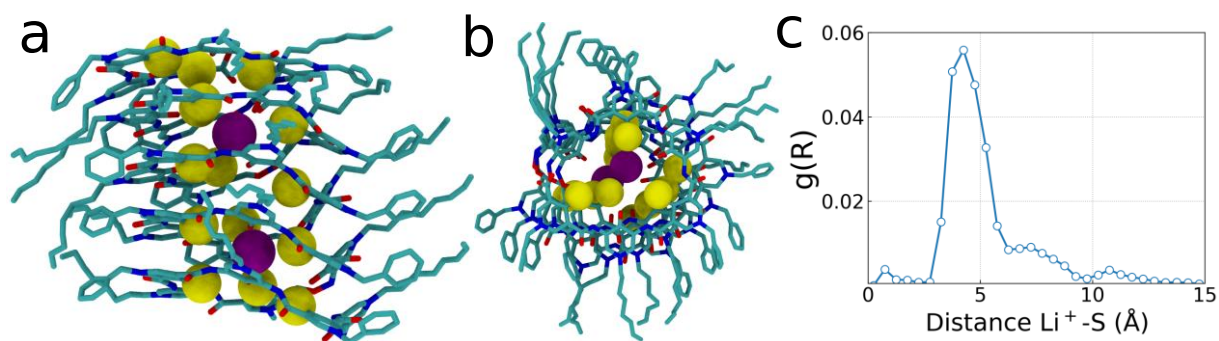
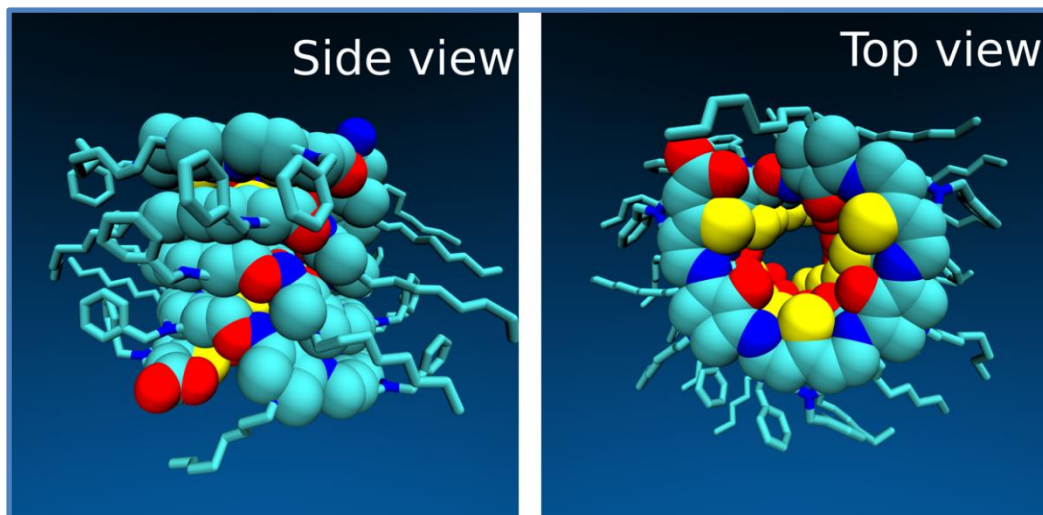
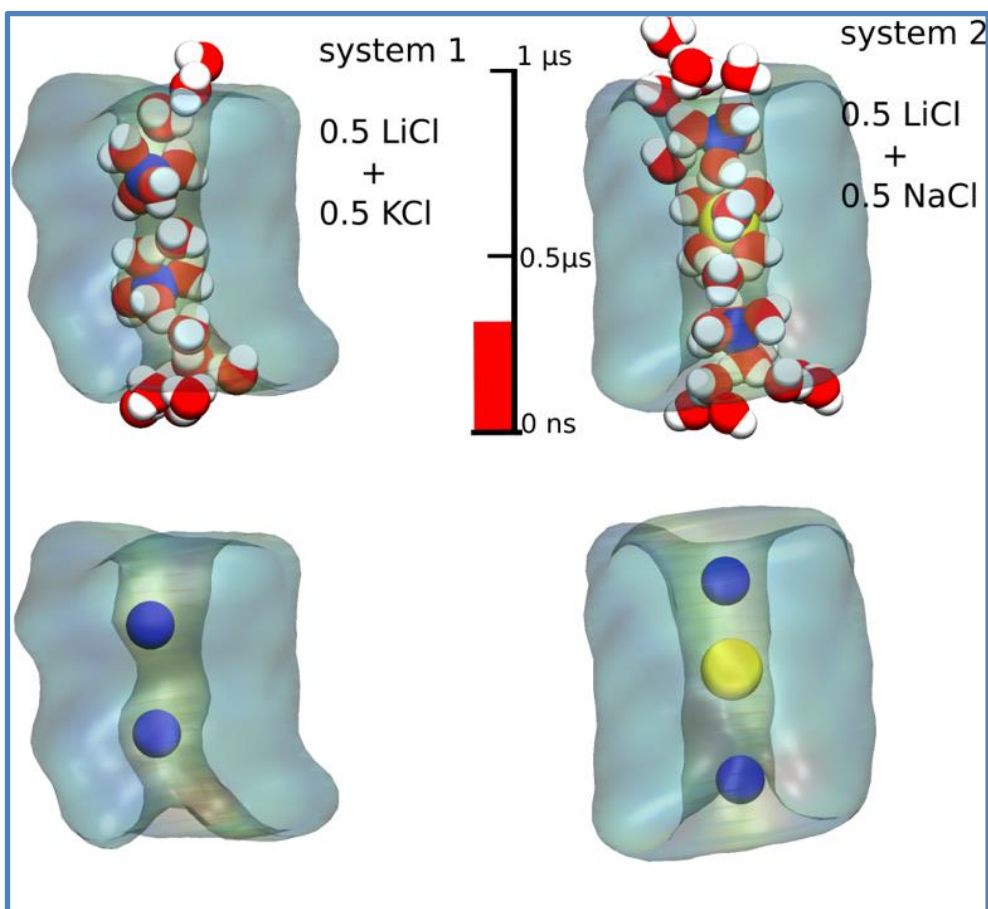


Figure S12: Hexagonal coordination of Li⁺ with the surrounding sulfur atoms (a) Top and (b) side views of a representative snapshot of the MD simulation trajectory, illustrating the Li⁺ ions (magenta) stabilized remotely and weakly by the surrounding sulfur atoms (yellow) present in the channel. During the long stay inside the channel, Li⁺ is surrounded by six sulfur atoms. (c) The radial distribution function of Li⁺ ions with the sulfur atoms of the P₁₅ channel wall showing a peak of about 5 Å in terms of Li⁺-S coordination distance.

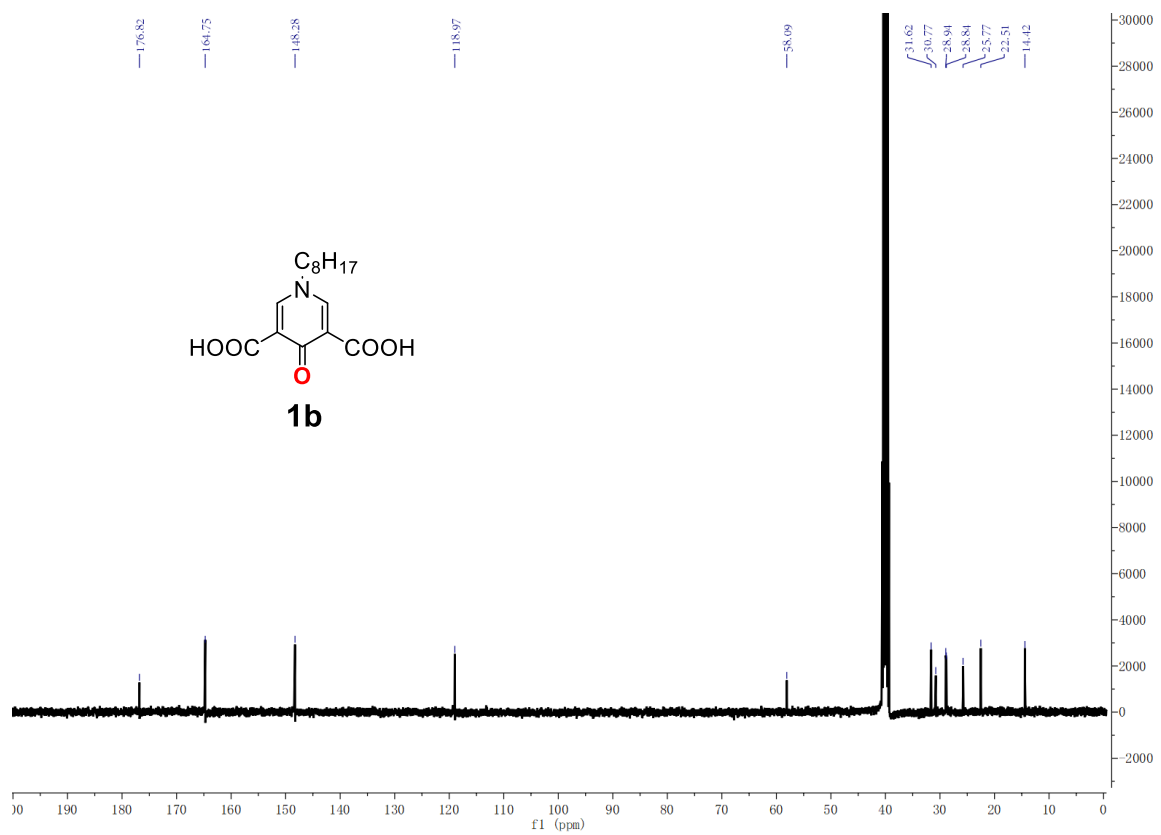
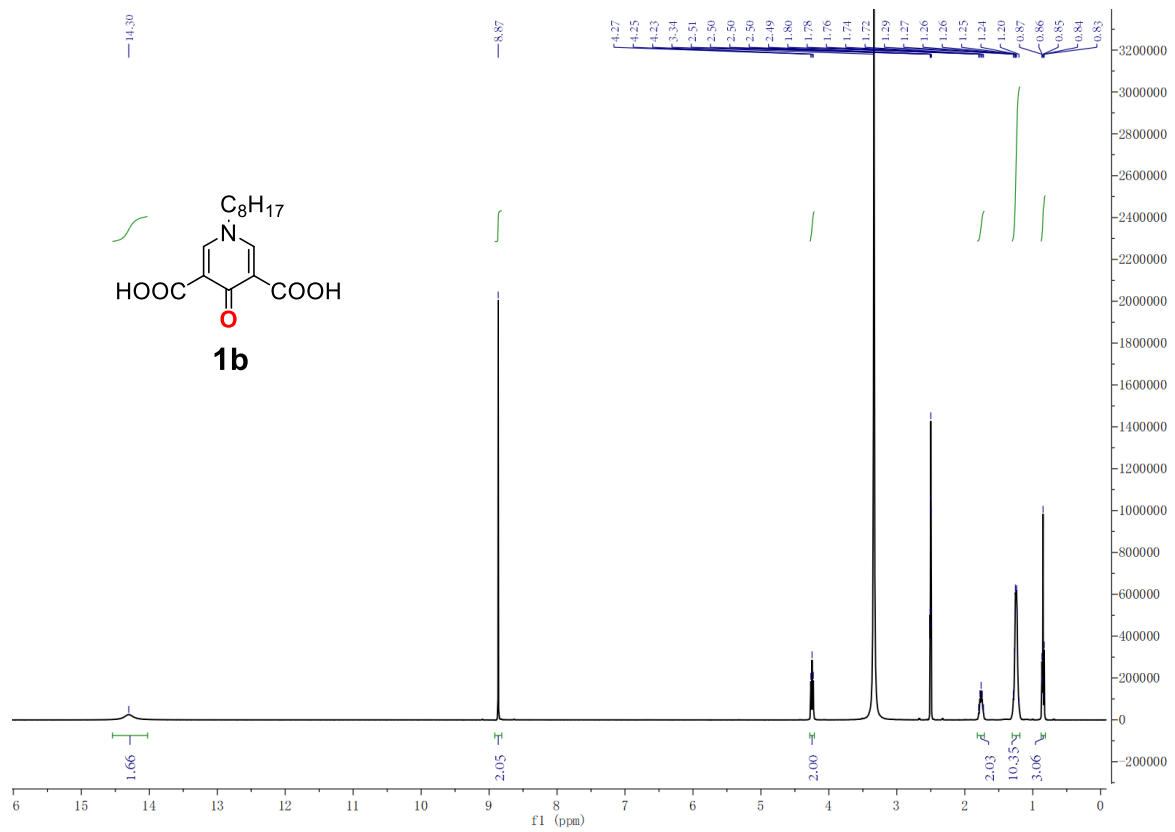


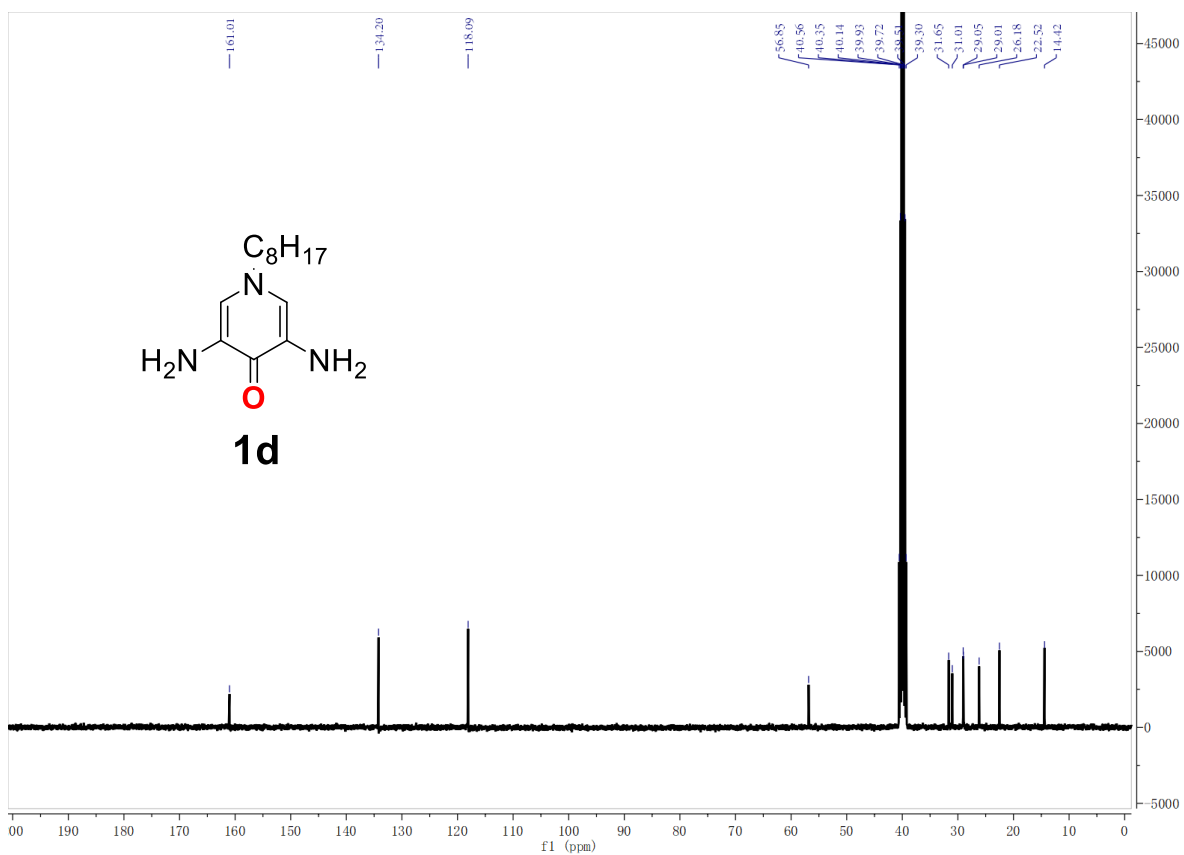
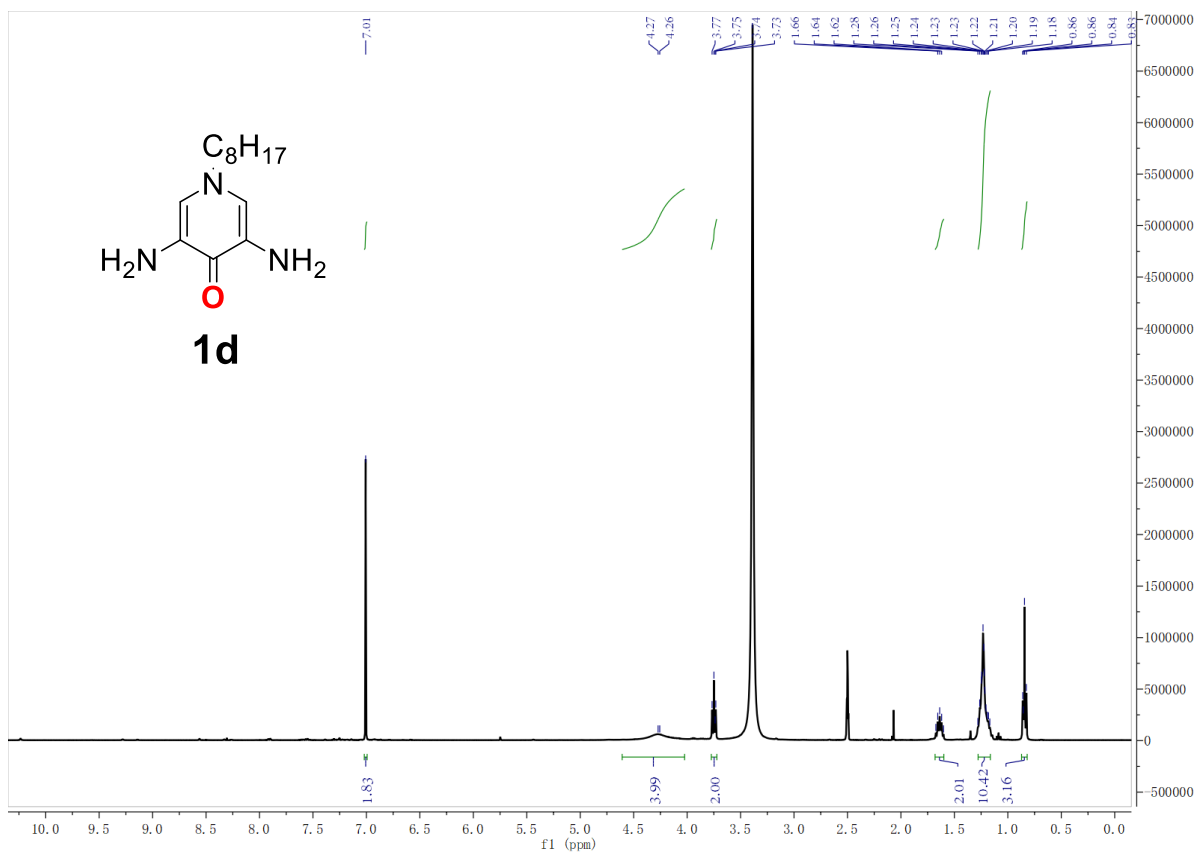
Supplementary Video SV1: 3D view of the all-atom model P₁₅ channel at the beginning of the simulation. The left panel shows a rotating side view, the right panel shows a zoom-in view passing inside the channel. C (turquoise), N (blue) S (yellow), and O (red) atoms around the central lumen of the channel are shown in using spheres whereas the rest of the non-hydrogen atoms are shown in licorice representation.

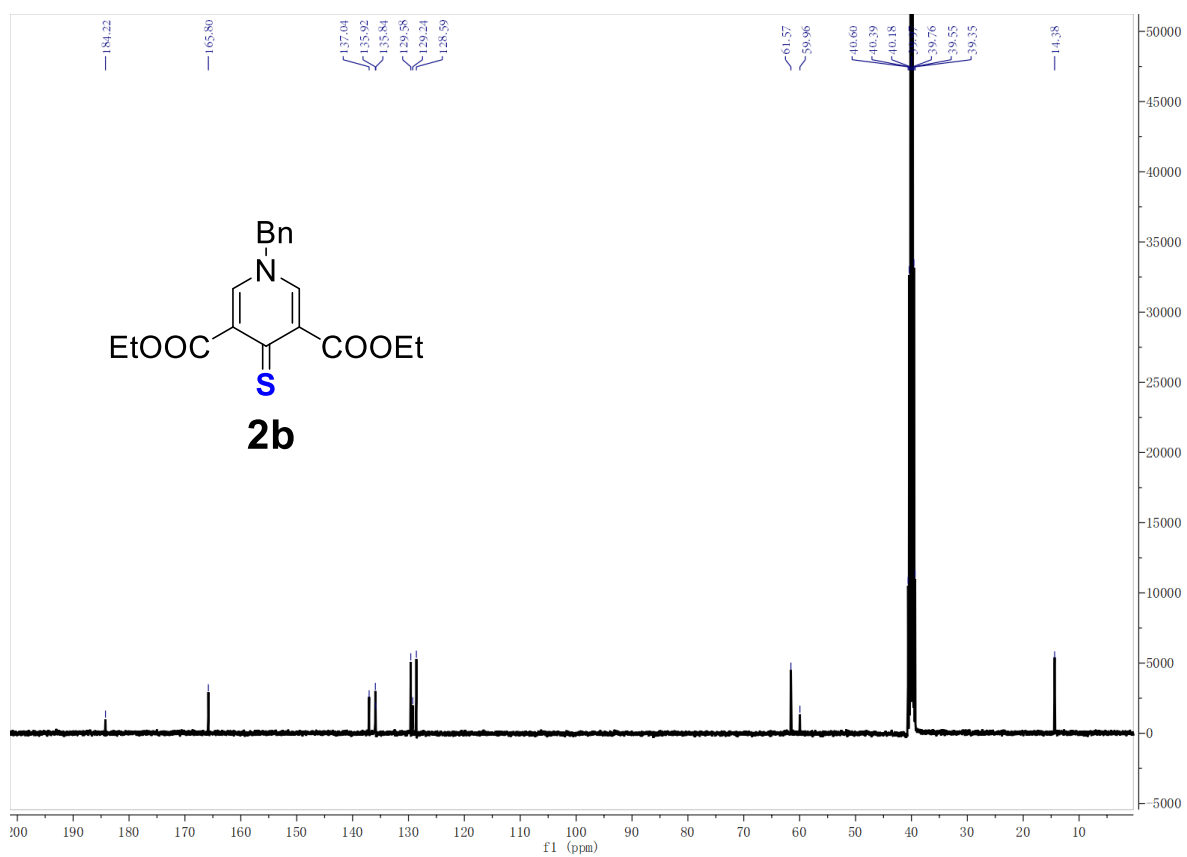
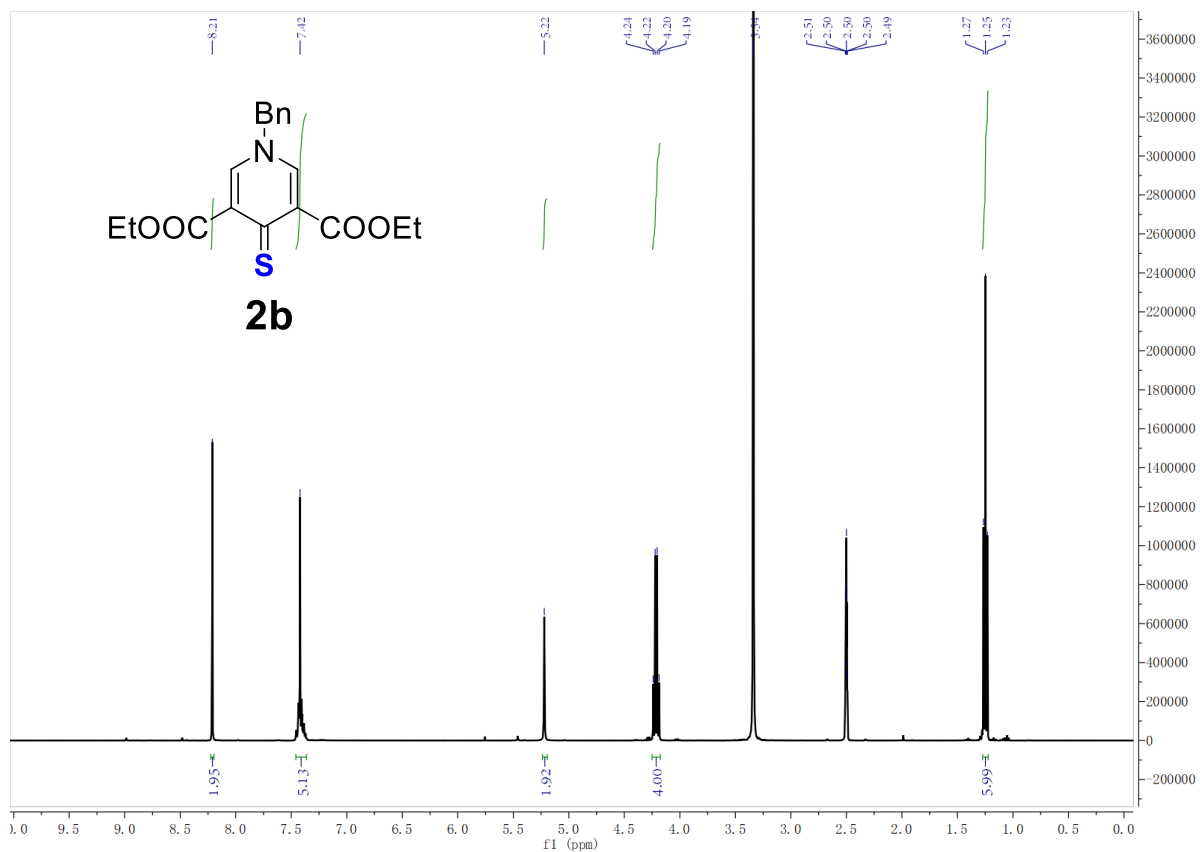


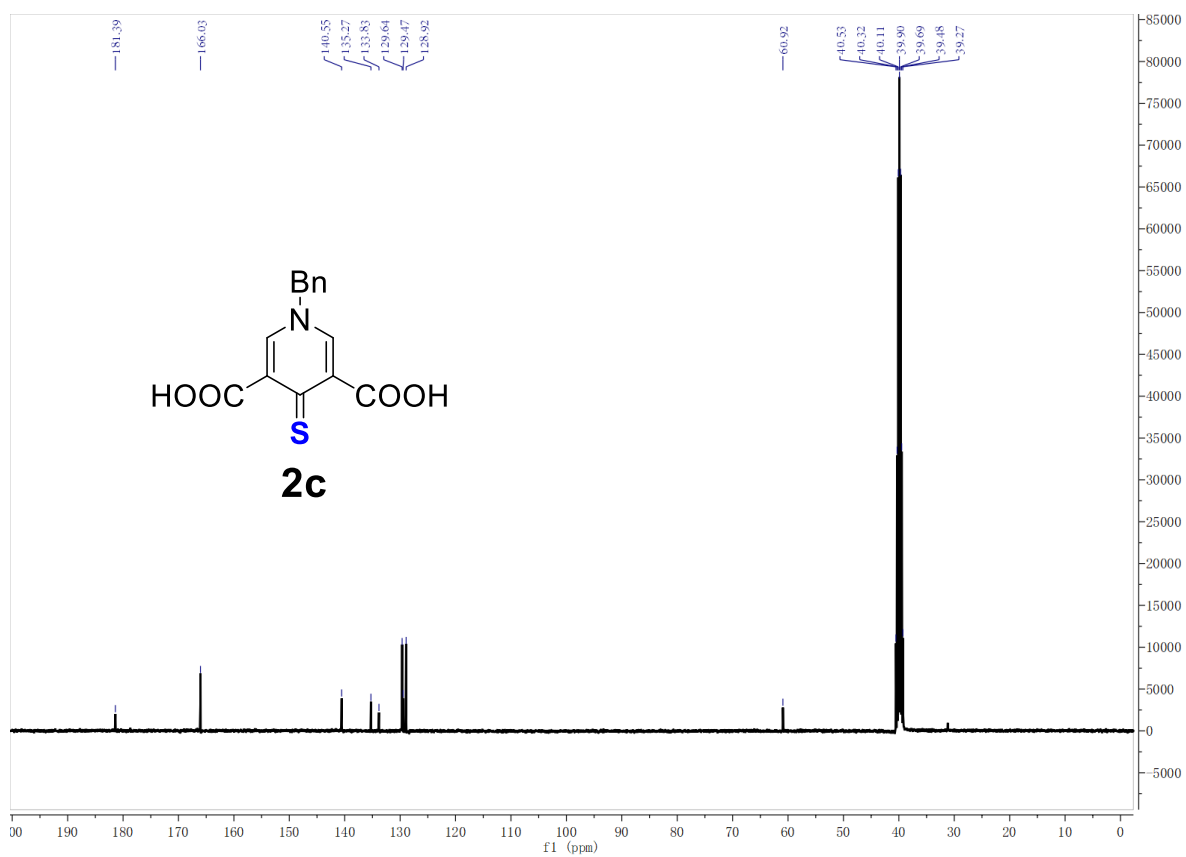
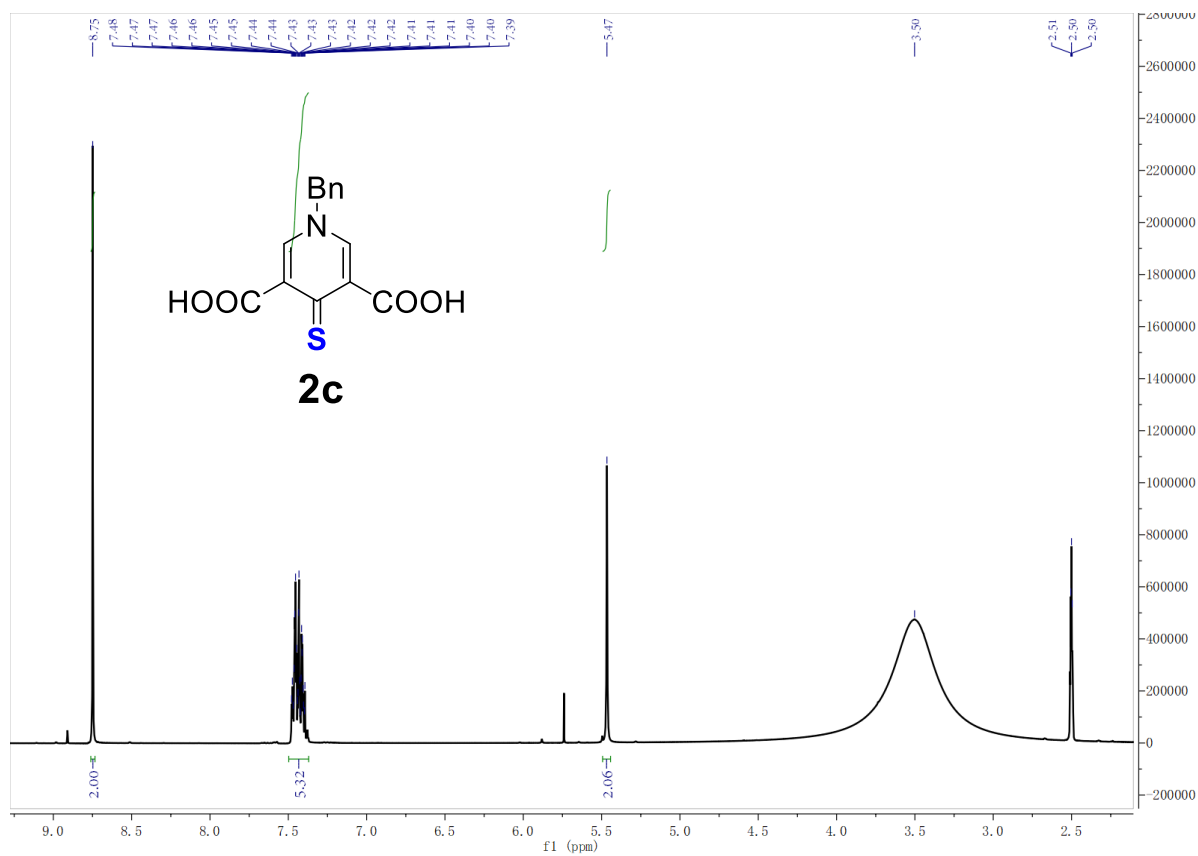
Supplementary Video SV2: Equilibrium MD simulation of P₁₅ channel in aqueous solution. One μ s long MD simulation trajectories of system 1 (left) and system 2 (right) showing a cut-away side view of the simulated systems. The movie illustrates the water (top) and (bottom) ion permeation through the P₁₅ channel. The atoms of the channel around the lumen are shown in surface representation, the water molecules present inside the channel are shown as red (O) and white (H) spheres. Ions present inside the channel, Li⁺ (blue), Na⁺ (yellow) and K⁺ (tan) are shown using spheres. The side chain of the channel, rest of the water and ions are not shown for the sake of clarity. The top row shows water and ion permeation through the channel in the equilibrium MD simulation, while in the same simulation trajectories shown in the bottom row water molecules are not shown for the sake of visualizing ion dynamics inside the channel.

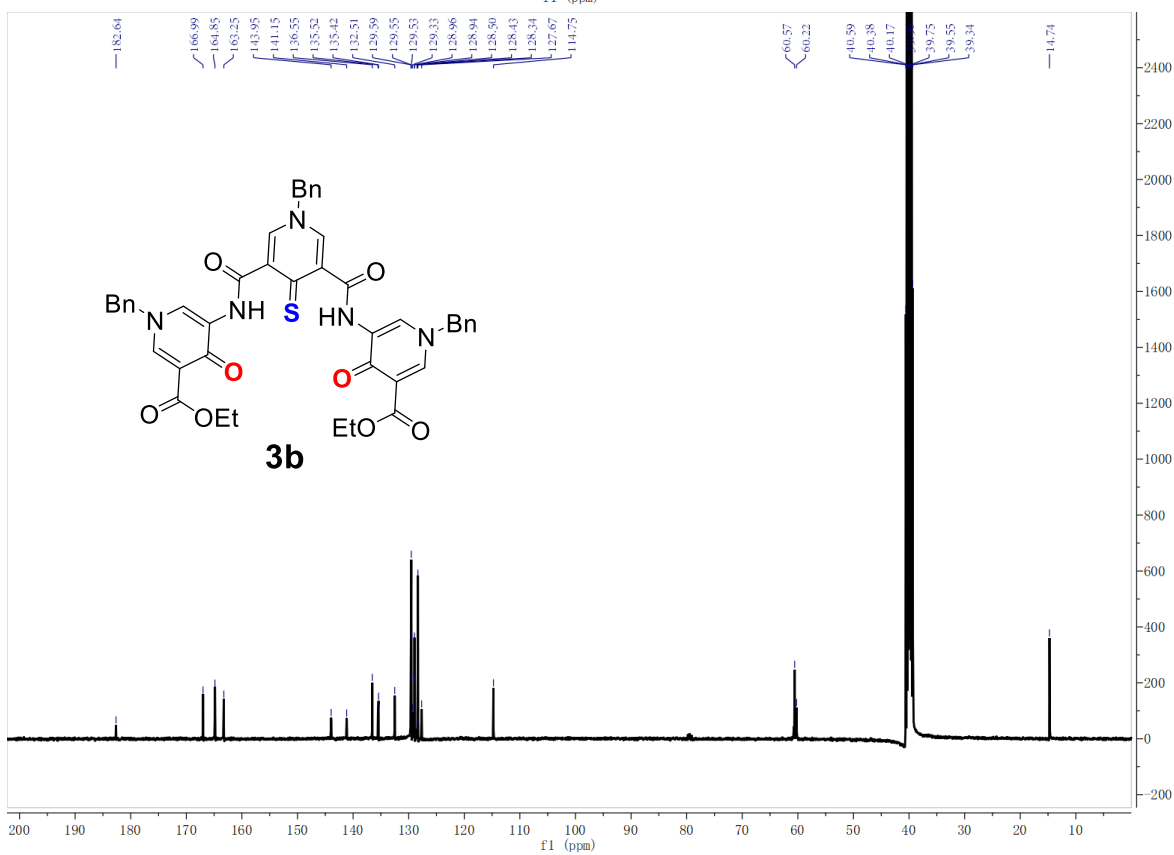
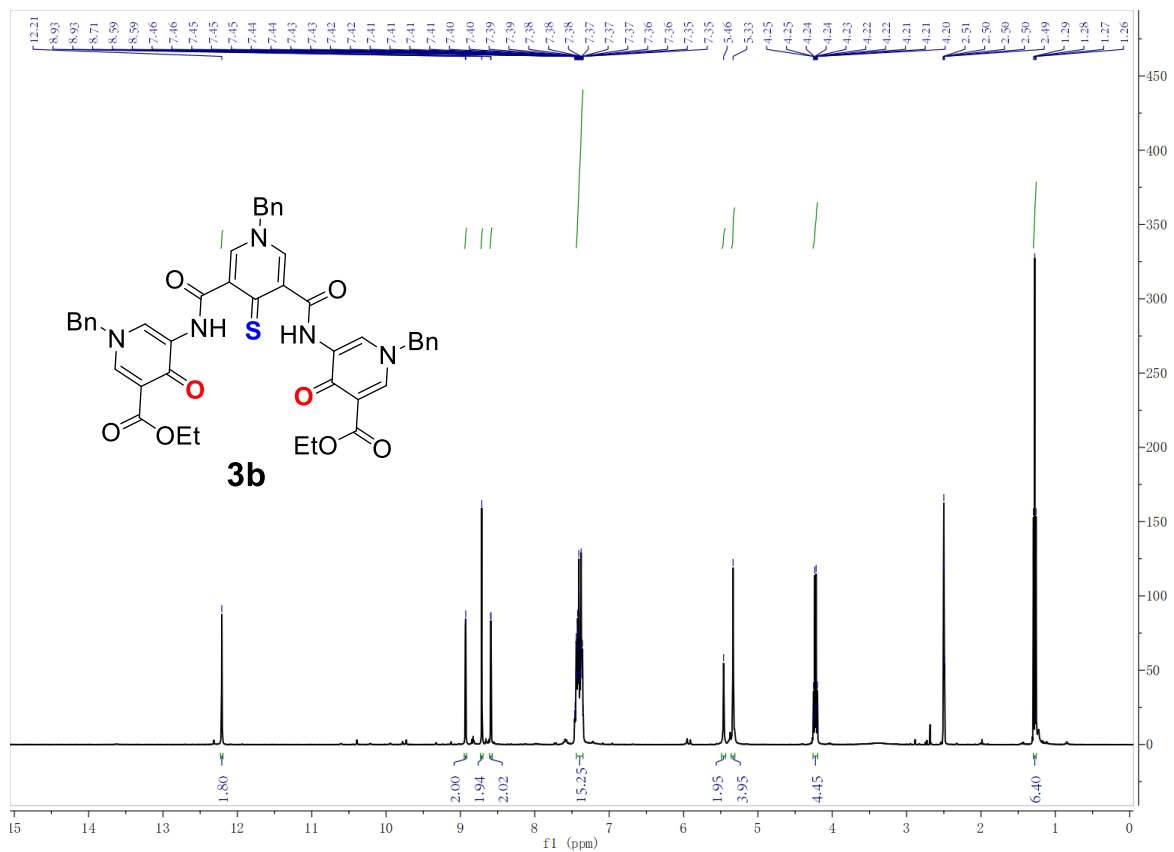
^1H and ^{13}C NMR Spectra











References

1. Phillips, J. C.; Hardy, D. J.; Maia, J. D.; Stone, J. E.; Ribeiro, J. V.; Bernardi, R. C.; Buch, R.; Fiorin, G.; Hénin, J.; Jiang, W., Scalable molecular dynamics on CPU and GPU architectures with NAMD. *J. Chem. Phys.* **2020**, *153* (4), 044130.
2. Mahler, J.; Persson, I., A study of the hydration of the alkali metal ions in aqueous solution. *Inorg. Chem.* **2012**, *51* (1), 425-438.
3. Sugita, Y.; Kitao, A.; Okamoto, Y., Multidimensional replica-exchange method for free-energy calculations. *J. Chem. Phys.* **2000**, *113* (15), 6042-6051.
4. Darden, T.; York, D.; Pedersen, L., Particle mesh ewald - An N.log(N) method for ewald sums in large systems. *J. Chem. Phys.* **1993**, *98* (12), 10089-10092.
5. Feller, S. E.; Zhang, Y.; Pastor, R. W.; Brooks, B. R., Constant pressure molecular dynamics simulation: the Langevin piston method. *J. Chem. Phys.* **1995**, *103* (11), 4613-4621.
6. Martyna, G. J.; Tobias, D. J.; Klein, M. L., Constant pressure molecular dynamics algorithms. *J. Chem. Phys.* **1994**, *101* (5), 4177-4189.
7. Sindhikara, D. J.; Kim, S.; Voter, A. F.; Roitberg, A. E., Bad seeds sprout perilous dynamics: Stochastic thermostat induced trajectory synchronization in biomolecules. *J. Chem. Theo. Comput.* **2009**, *5* (6), 1624-1631.
8. Klauda, J. B.; Venable, R. M.; Freites, J. A.; O'Connor, J. W.; Tobias, D. J.; Mondragon-Ramirez, C.; Vorobyov, I.; MacKerell Jr, A. D.; Pastor, R. W., Update of the CHARMM all-atom additive force field for lipids: validation on six lipid types. *J. Phys. Chem. Lett. B* **2010**, *114* (23), 7830-7843.
9. Beglov, D.; Roux, B., Finite representation of an infinite bulk system: solvent boundary potential for computer simulations. *J. Chem. Phys.* **1994**, *100* (12), 9050-9063.
10. Yoo, J.; Aksimentiev, A., Improved parametrization of Li⁺, Na⁺, K⁺, and Mg²⁺ ions for all-atom molecular dynamics simulations of nucleic acid systems. *J. Phys. Chem. Lett.* **2012**, *3* (1), 45-50.
11. Yoo, J.; Aksimentiev, A., New tricks for old dogs: improving the accuracy of biomolecular force fields by pair-specific corrections to non-bonded interactions. *Phys. Chem. Chem. Phys.* **2018**, *20* (13), 8432-8449.
12. Miyamoto, S.; Kollman, P. A., Settle: An analytical version of the SHAKE and RATTLE algorithm for rigid water models. *J. Comput. Chem.* **1992**, *13* (8), 952-962.

13. Andersen, H. C., Rattle: A “velocity” version of the shake algorithm for molecular dynamics calculations. *J. Comput. Chem.* **1983**, *52* (1), 24-34.
14. Humphrey, W.; Dalke, A.; Schulten, K., VMD: Visual molecular dynamics. *J. Mol. Graph.* **1996**, *14* (1), 33-38.
15. Roe, D. R.; Cheatham, T. E., III, PTRAJ and CPPTRAJ: Software for Processing and Analysis of Molecular Dynamics Trajectory Data. *J. Chem. Theo. Comput.* **2013**, *9* (7), 3084-3095.
16. Vanommeslaeghe, K.; Hatcher, E.; Acharya, C.; Kundu, S.; Zhong, S.; Shim, J.; Darian, E.; Guvench, O.; Lopes, P.; Vorobyov, I., CHARMM general force field: A force field for drug-like molecules compatible with the CHARMM all-atom additive biological force fields. *J. Comput. Chem.* **2010**, *31* (4), 671-690.
17. Torrie, G. M.; Valleau, J. P., Nonphysical sampling distributions in Monte Carlo free-energy estimation: Umbrella sampling. *J. Comput. Phys.* **1977**, *23* (2), 187-199.
18. Kumar, S.; Rosenberg, J. M.; Bouzida, D.; Swendsen, R. H.; Kollman, P. A., The weighted histogram analysis method for free-energy calculations on biomolecules. I. The method. *J. Comput. Chem.* **1992**, *13* (8), 1011-1021.
19. Jo, S.; Kim, T.; Iyer, V. G.; Im, W., CHARMM-GUI: a web-based graphical user interface for CHARMM. *J. Comput. Chem.* **2008**, *29* (11), 1859-1865.
20. Jorgensen, W. L.; Chandrasekhar, J.; Madura, J. D.; Impey, R. W.; Klein, M. L., Comparison of simple potential function for simulating liquid water. *J. Chem. Phys.* **1983**, *79* (2), 926-935.
21. Smart, O. S.; Neduvilil, J. G.; Wang, X.; Wallace, B.; Sansom, M. S., HOLE: a program for the analysis of the pore dimensions of ion channel structural models. *J. Mol. Graph.* **1996**, *14* (6), 354-360.